Supplement of

A new model mechanism for atmospheric oxidation of isoprene: global effects on oxidants, nitrogen oxides, organic products, and secondary organic aerosol

Kelvin H. Bates and Daniel J. Jacob

Correspondence to: Kelvin H. Bates (kelvin_bates@fas.harvard.edu)

Contents

S1 Additional details from global simulations

Tables S1-S3 provide additional details from global simulations of RCIM. Tables S1-S2 show the percent changes in global annual average tropospheric burdens of compounds of interest between a standard global simulation and a perturbed simulation. Perturbations include removing isoprene chemistry altogether, using the GEOS-Chem v11-02c mechanism, and using the RCIM with different ISOPOO isomer branchings.

Table S1 also shows changes due to the removal of specific isoprene and ISOPOO reaction pathways (e.g. isoprene + O_3 or ISOPOO + RO_2), which gives a sense of the specific contributions of these pathways to the overall tropospheric effects of isoprene oxidation. Table S2 shows similar perturbations but with specific oxidation products (e.g. MVK, IEPOX) removed, which gives a sense of those products' contributions to isoprene's tropospheric effects, as well as perturbations to isoprene nitrate chemistry. Table S3 provides global annual average molar yields of VOCs from isoprene, using both RCIM and GEOS-Chem v11-02c, as well regional molar yields in the southeastern United States, the Amazon, and eastern China using RCIM.

Table S1: Percent changes in annual average tropospheric mixing ratios due to specific perturbations to the isoprene oxidation mechanism.

Species	No isoprene	Fixed ISOPOO distrib.[a]	Single ISOPOO species[b]	No isoprene + O_3[c]	No isoprene + NO_3[c]	No ISOPOO + NO[c]	No ISOPOO + HO_2[c]	No ISOPOO H-shifts[c]	No ISOPOO + RO_2[c]
OH	12.9	1.27	0.03	1.15	-0.17	6.64	3.36	-1.23	0.59
HO_2	-6.15	0.60	-0.20	-1.12	-0.26	-2.85	0.17	-1.81	-0.96
NO	6.23	0.72	0.07	0.36	0.00	6.25	1.03	-1.28	0.23
NO_2	3.04	0.49	0.28	0.00	-0.38	5.74	0.45	-0.43	-0.02
NO_3	10.4	2.30	-0.41	-0.13	3.47	5.11	7.15	-5.46	-0.54
O_3	-3.37	0.50	0.04	-0.22	-0.40	-0.30	-0.40	-1.28	-0.42
CO	-24.1	-0.23	-0.55	-3.05	-0.40	-10.8	-6.00	-2.33	-1.99
Formaldehyde	-17.4	-0.05	-1.26	-4.37	-0.94	-7.59	-3.10	-2.50	-2.68
Formic acid	-94.2	-6.01	1.20	-48.4	-4.16	-32.6	-13.3	19.2	-4.40
Acetic acid	-58.6	4.51	-3.05	-4.28	-1.32	-25.4	-9.51	-12.5	-5.41
Glycolaldehyde	-97.6	-17.0	-14.8	-5.82	-3.80	-62.6	-24.8	-0.33	-11.9
Glyoxal	-43.1	44.1	-17.6	-1.27	-1.07	-14.0	-4.78	-17.2	-1.74
Hydroxyacetone	-89.9	-2.10	20.8	-16.8	-1.55	-42.1	-30.8	-1.11	-11.24
Methylglyoxal	-87.3	5.30	-5.78	-5.78	-2.37	-32.1	-15.8	-37.9	-6.12
Methyl vinyl ketone	-100	-24.3	-17.3	-11.3	-2.50	-63.3	-29.2	10.5	-21.2
Methacrolein	-99.3	-3.22	23.4	-35.0	-1.39	-45.3	-20.5	32.8	-20.0
PANs[d]	-18.7	-0.74	-0.42	-1.76	-1.74	-10.28	-5.96	-0.82	-2.20
C_{2+} nitrates[d,e]	-97.4	-1.91	22.5	-9.96	-38.6	-24.3	-1.24	9.91	-4.32
C_{2+} hydroperoxides[d]	-100	-13.8	4.68	-4.27	-1.08	-38.4	-82.0	-8.67	-9.21
Epoxides[d]	-99.5	-7.16	1.99	-4.98	-0.65	-32.9	-89.4	-8.3	-5.0
Tetrafunctionals[d]	-100	-2.39	10.4	-1.71	-4.3	-21.3	-82.7	15.9	-0.45
CH_4 lifetime	-13.6	-1.58	0.06	-1.12	0.27	-6.47	-3.42	1.57	-0.53

All listed changes are relative to a simulation employing RCIM, from $4° \times 5°$ horizontal resolution global simulations. [a]from Paulot et al. (2009); [b]as in GEOS-Chem v10-01 (Mao et al., 2013); [c]in these comparisons, the reaction in question remains in the mechanism with its standard rate, but forms no products and does not consume the co-reactant; [d]percent differences in lumped classes of compounds are calculated by mole, not mass; [e]includes only non-PAN organonitrates.

Table S2: Percent changes in annual average tropospheric mixing ratios due to specific perturbations to the isoprene oxidation mechanism.

Species	No isoprene	No MVK[a]	No MCAR[a]	No IEPOX[a]	No isoprene hydroxy-nitrates[a]	Full nitrate removal[b]	Slow nitrate hydrolysis[c]
OH	12.9	1.35	0.86	1.46	-0.48	-15.7	0.99
HO_2	-6.15	-2.41	-1.20	-0.09	0.13	-4.27	0.32
NO	6.23	1.73	0.61	0.58	-0.47	-9.24	0.70
NO_2	3.04	0.28	-0.03	0.26	-0.41	-10.5	0.78
NO_3	10.4	-3.64	-1.63	4.72	0.74	-22.3	2.21
O_3	-3.37	-1.88	-1.01	-0.18	-0.43	-12.2	0.82
CO	-24.1	-5.11	-3.03	-2.58	0.18	9.63	-0.49
Formaldehyde	-17.4	-5.58	-2.23	-0.46	-0.48	-14.0	0.71
Formic acid	-94.2	-33.6	-10.3	-3.42	-1.47	-25.9	2.48
Acetic acid	-58.6	-19.5	-10.1	-4.23	0.26	-5.25	0.58
Glycolaldehyde	-97.6	-87.4	0.43	-3.18	-1.74	-39.0	3.45
Glyoxal	-43.1	-18.3	0.53	-0.72	1.46	-1.06	1.07
Hydroxyacetone	-89.9	-6.52	-54.5	-15.5	0.38	10.3	1.19
Methylglyoxal	-87.3	-28.4	-12.8	-6.55	-0.48	-16.9	1.44
Methyl vinyl ketone	-100	-2.24	-1.65	-3.40	-0.22	2.67	-1.36
Methacrolein	-99.3	-4.24	-3.35	-4.04	-0.14	27.1	-1.71
PANs[d]	-18.7	-15.0	-5.35	-2.53	-1.00	-25.0	1.87
C_{2+} nitrates[d,e]	-97.4	-8.02	-41.7	2.23	-6.75	-53.7	32.1
C_{2+} hydroperoxides[d]	-100	-7.96	-2.61	-0.49	1.41	51.5	-1.88
Epoxides[d]	-99.5	-5.07	-10.4	3.89	2.08	24.4	-0.25
Tetrafunctionals[d]	-100	-2.81	-1.40	18.5	-3.22	21.6	16.9
CH_4 lifetime	-13.6	-1.22	-0.80	-1.50	0.51	20.5	-1.04

All listed changes are relative to a simulation employing RCIM, from $4° \times 5°$ horizontal resolution global simulations. [a]in these comparisons, the species in question is still produced in the isoprene oxidation mechanism, but is not allowed to react; [b]this simulation assumes the limiting case that all ISOPOO + NO reactions lead to the formation of non-NO_x recycling nitrates; [c]referring only to the 1-OH,2-ONO_2 isoprene hydroxynitrate, the heterogeneous hydrolysis rate of which is reduced by an order of magnitude for this comparison; [d]percent differences in lumped classes of compounds are calculated by mole, not mass; [e]includes only non-PAN organonitrates.

S3

Table S3: Molar yields of VOCs and SOA precursors of interest from isoprene[a]

Species	Molar yield from isoprene, %, RCIM (GEOS-Chem v11-02c)			
	Global	SE USA	Amazon	E China
CO	190 (180)	150 (121)	138 (101)	213 (197)
Formaldehyde	111 (107)	97.7 (77.0)	79.4 (44.3)	148 (141)
Formic acid	5.76 (6.33)	5.28 (4.53)	4.12 (4.05)	7.59 (7.05)
Acetic acid	5.49 (4.18)	2.93 (2.04)	3.34 (2.59)	4.59 (3.11)
Hydroxymethyl hydroperoxide	3.94 (-)	4.55 (-)	4.71 (-)	2.53 (-)
Glycolaldehyde	11.5 (16.2)	11.1 (13.41)	5.00 (12.1)	23.7 (20.1)
Glyoxal	1.63 (5.47)	1.06 (3.85)	1.08 (2.17)	2.06 (6.51)
Hydroxyacetone	12.3 (11.1)	10.6 (10.0)	7.72 (5.00)	15.2 (17.2)
Methylglyoxal	20.1 (24.5)	16.1 (18.2)	13.4 (15.3)	25.3 (29.3)
Methyl vinyl ketone	27.9 (21.5)	31.1 (25.7)	22.0 (15.5)	42.2 (35.8)
Methacrolein	15.9 (17.3)	17.9 (20.6)	15.1 (14.2)	21.3 (26.5)
C_4 dihydroxycarbonyls	6.32 (3.67)	4.99 (2.31)	3.59 (1.86)	4.58 (2.85)
C_4 hydroxydicarbonyls	10.6 (-)	7.60 (-)	6.49 (-)	8.43 (-)
C_{2+} nitrates[c,d]	5.99 (6.96)	9.08 (9.95)	1.30 (1.09)	15.1 (19.1)
$\quad$ C_5 nitrates[c]	4.82 (4.79)	7.55 (7.16)	1.02 (0.848)	11.8 (11.9)
$\quad$ C_5 hydroxynitrates	3.60 (2.61)	5.31 (3.82)	0.782 (0.488)	9.25 (6.68)
$\quad$ C_4 nitrates[c]	0.878 (1.70)	1.10 (2.03)	0.234 (0.185)	2.42 (5.85)
$\quad$ Propanone nitrate	0.188 (0.412)	0.304 (0.675)	0.0277 (0.0483)	0.627 (1.20)
C_{2+} hydroperoxides[c]	52.3 (42.6)	43.9 (33.1)	58.7 (47.2)	24.9 (18.1)
$\quad$ ISOPOOH	35.3 (33.8)	29.7 (29.7)	41.2 (37.1)	14.0 (13.8)
$\quad$ C_5 hydroperoxy aldehydes	6.77 (5.80)	4.93 (3.56)	8.49 (7.89)	3.42 (2.08)
Epoxides[c]	25.7 (25.8)	23.3 (21.4)	20.9 (18.1)	15.3 (20.9)
$\quad$ IEPOX	20.1 (19.9)	18.3 (16.8)	17.1 (15.7)	9.84 (10.5)
$\quad$ HMML	0.732 (5.85)	0.937 (4.62)	0.154 (2.40)	2.42 (10.3)
Tetrafunctionals[c]	4.07 (4.11)	3.73 (3.32)	3.26 (3.80)	2.63 (3.62)
$\quad$ IDHPE[e]	2.20 (-)	1.86 (-)	2.12 (-)	0.847 (-)
$\quad$ IDHDP[f]	0.530 (0.0992)	0.438 (0.0808)	0.486 (0.0830)	0.159 (0.0480)
$\quad$ ICPDH[g]	0.458 (0.584)	0.346 (0.341)	0.380 (0.719)	0.185 (0.149)
$\quad$ IDCHP[h]	0.384 (-)	0.349 (-)	0.190 (-)	0.359 (-)
$\quad$ ICHNP[i]	0.232 (-)	0.319 (-)	0.0353 (-)	0.479 (-)
$\quad$ IDHPN[j]	0.218 (0.466)	0.348 (0.538)	0.0386 (0.0890)	0.411 (0.596)

[a]Results from $2° \times 2.5°$ horizontal resolution global simulations using RCIM. Yields of species with additional non-isoprene precursors are calculated by taking the difference in production between a simulation with isoprene and one without isoprene emissions. Yields of CO and formaldehyde calculated with this method are then corrected for differences in total methane oxidation between the simulations. [b]Using the GEOS-Chem v11-02c mechanism instead of RCIM. [c]Yields of lumped species may include multiple generations of a single oxidation pathway (e.g., separately counting both IEPOX and its oxidation product, isoprene hydroxycarbonyl epoxides). [d]Includes only non-PAN organonitrates. [e]C_5 dihydroxy-hydroperoxy-epoxides. [f]C_5 dihydroxy-dihydroperoxides. [g]C_5 dihydroxy-carbonyl-hydroperoxides. [h]C_5 dicarbonyl-hydroxy-hydroperoxides. [i]C_5 carbonyl-hydroxy-hydroperoxy-nitrates. [j]C_5 dihydroxy-hydroperoxy-nitrates.

S2   Light & temperature sensitivities in fixed-radical box models

Figures S1-S5 show the effects of varying light and temperature on HO_x, ozone, oxidation pathways, and VOC yields in fixed-radical box models. In addition to the simulations described in the main text, the model was run with every permutation of (a) temperature set to 283.15 K, 298.15 K, and 313.15 K, and (b) solar radiation for photolysis set to clear-sky equatorial midday with an ozone column of 350 DU, 0.1×equatorial midday, and 0. The primary effect of temperature is to increase the rates of H-shift reactions, which substantially increases their relative contribution to the fate of the ISOPOO radicals (Figure S1). This leads to an increase in overall net HO_x recycling from isoprene oxidation (Figure S2). Increased photolysis rates from higher photon fluxes also lead to increased net HO_x recycling (Figure S2) and net potential ozone production (Figure S3) from isoprene oxidation.

    The effects of temperature on VOC yields (Figure S4) are largely mediated by the temperature dependence of H-shift reactions (Peeters and Nguyen, 2012; Peeters et al., 2014; Crounse et al., 2011; Praske et al., 2018) and of nitrate formation branching ratios in reactions of peroxy radicals with NO (Arey et al., 2001; Carter and Atkinson, 1985, 1989). Thus, overall yields from isoprene of ISOPOO H-shift products (e.g. C_2-C_5 hydroperoxyaldehydes) increase with temperature, while those of organonitrates decrease. The effects of light on VOC yields (Figure S5) are generally smaller than those of temperature, but among the most pronounced are a decrease in formaldehyde yields and an increase in methylglyoxal yields under low-light conditions.
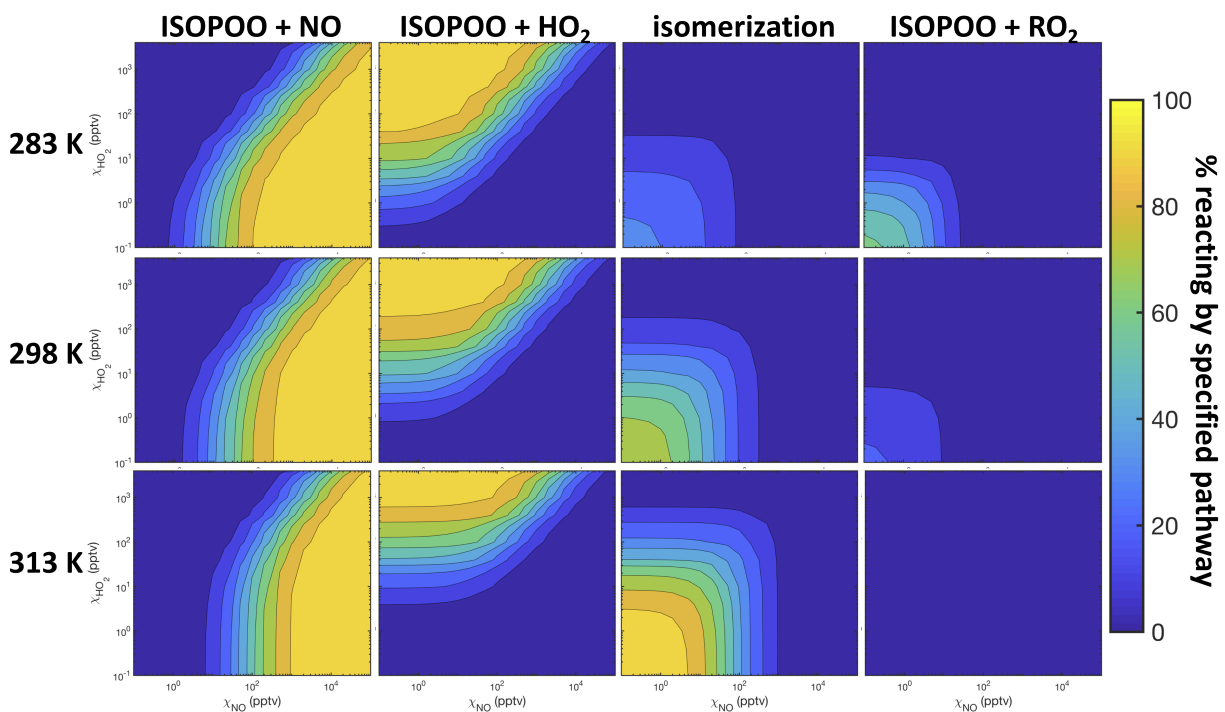

Figure S1: Temperature dependence of the percent of isoprene hydroxy peroxy radicals reacting via each pathway as a function of NO and HO_2, from fixed-radical box modeling of RCIM.
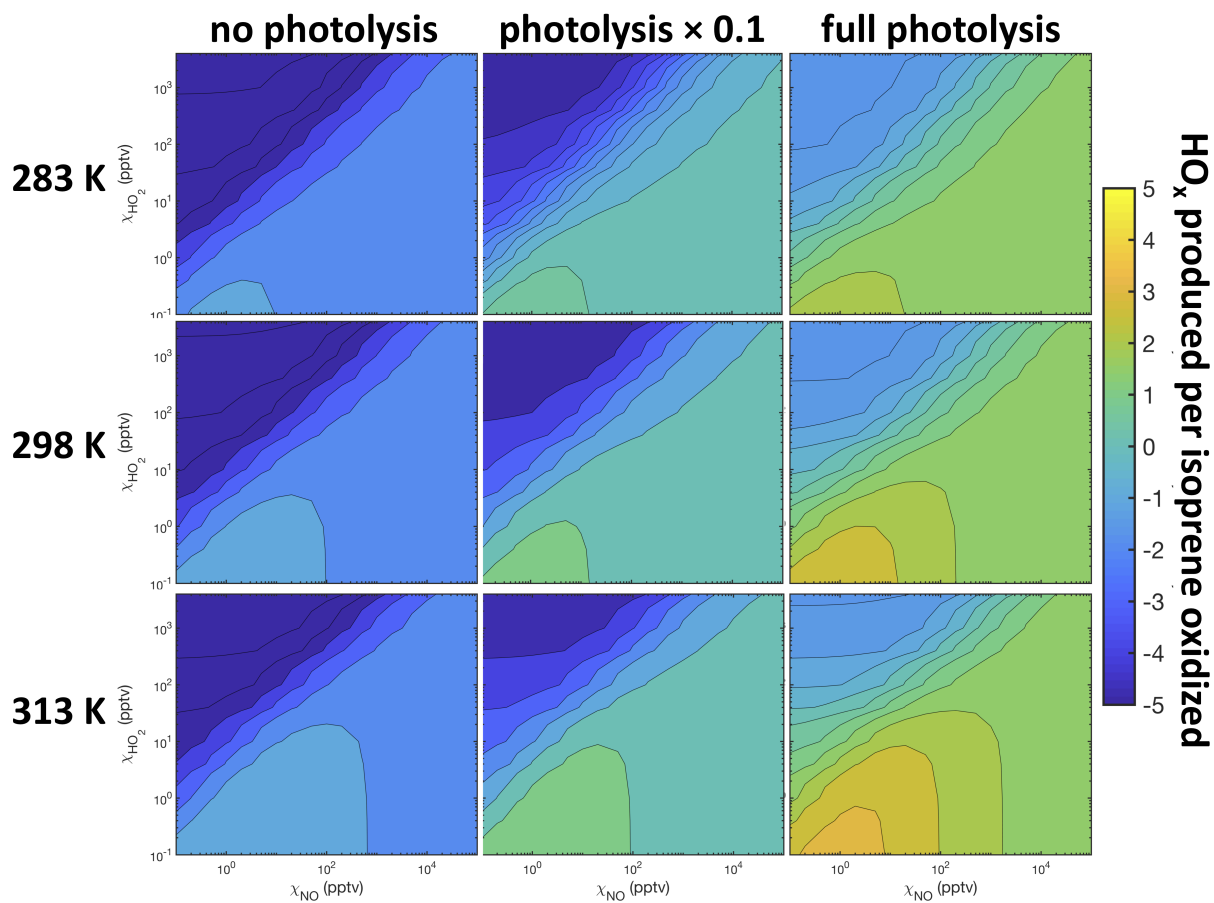
Figure S2: Net effects of isoprene oxidation on HO_x under various temperature and light conditions as a function of NO and HO_2, from fixed-radical box modeling of RCIM.
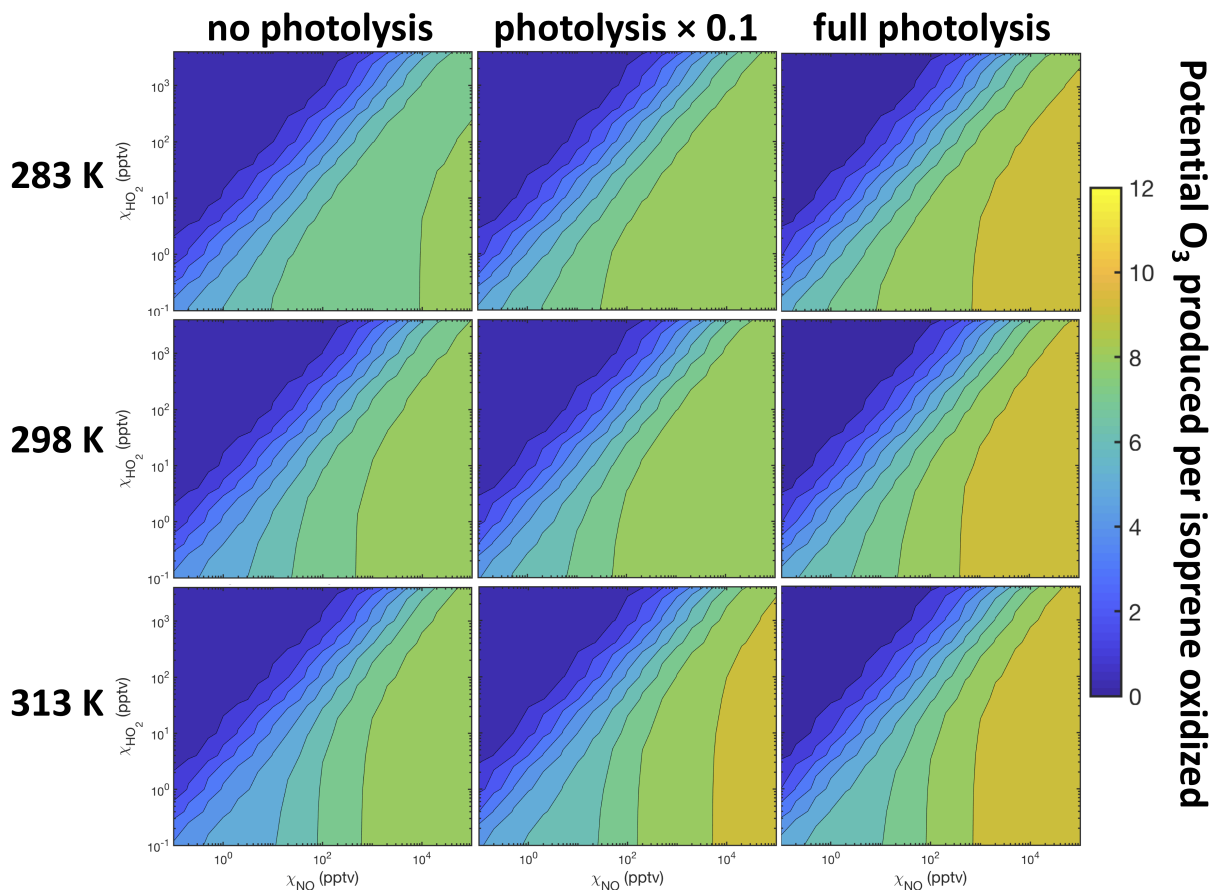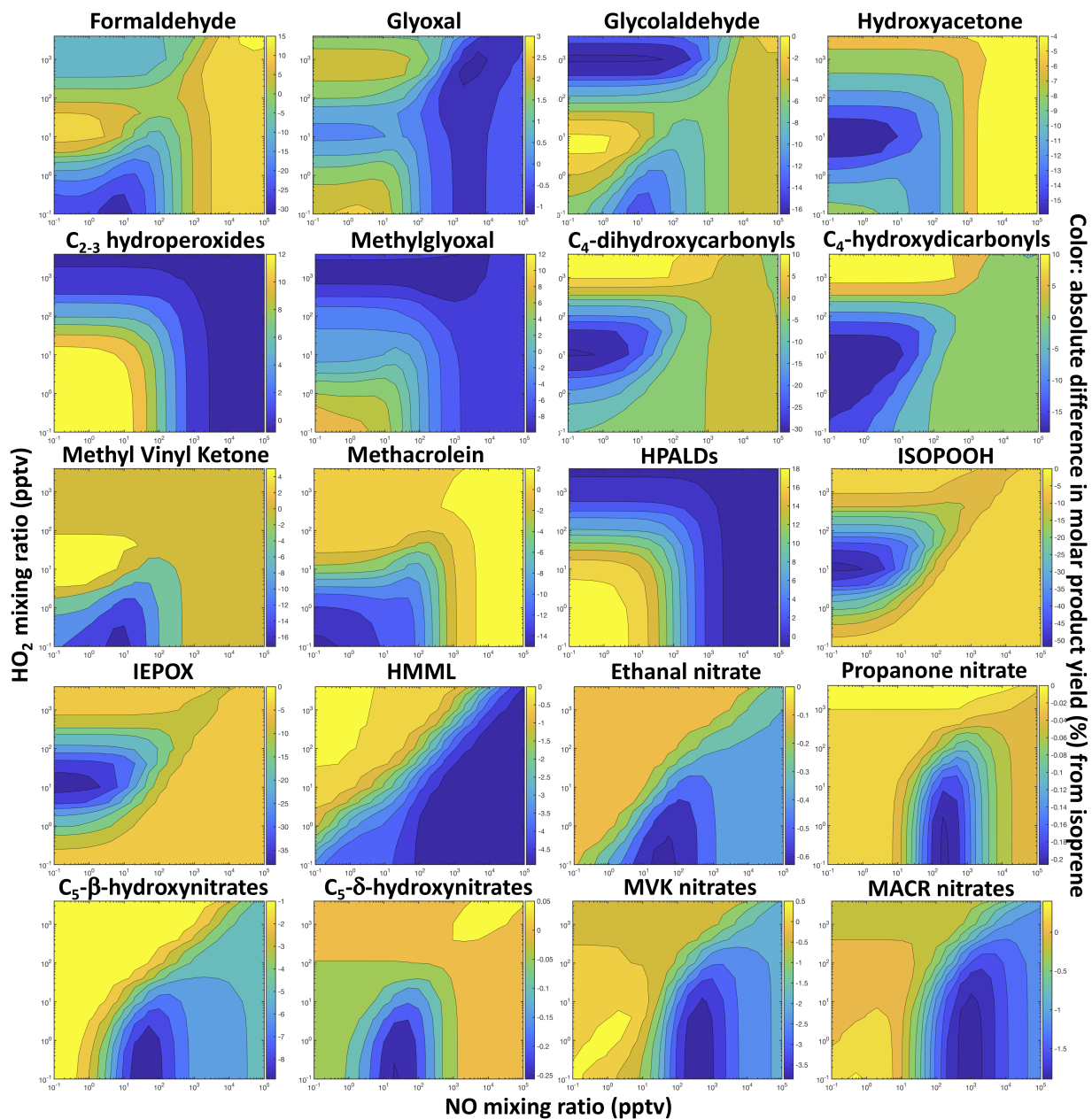
Figure S3: Net effects of isoprene oxidation on potential O_3 – estimated as the sum of the ozone, NO_2, and HO_2 (times the fraction of HO_2 that would go on to react with NO) produced over the course of its oxidation – under various temperature and light conditions as a function of NO and HO_2, from fixed-radical box modeling of RCIM.

Figure S4: Absolute changes in percent yields of compounds of interest from isoprene when switching from fixed-radical box models run at 10 °C to simulations run at 40 °C. All box models are run with full photolytic sunlight flux (equatorial midday) and using RCIM.
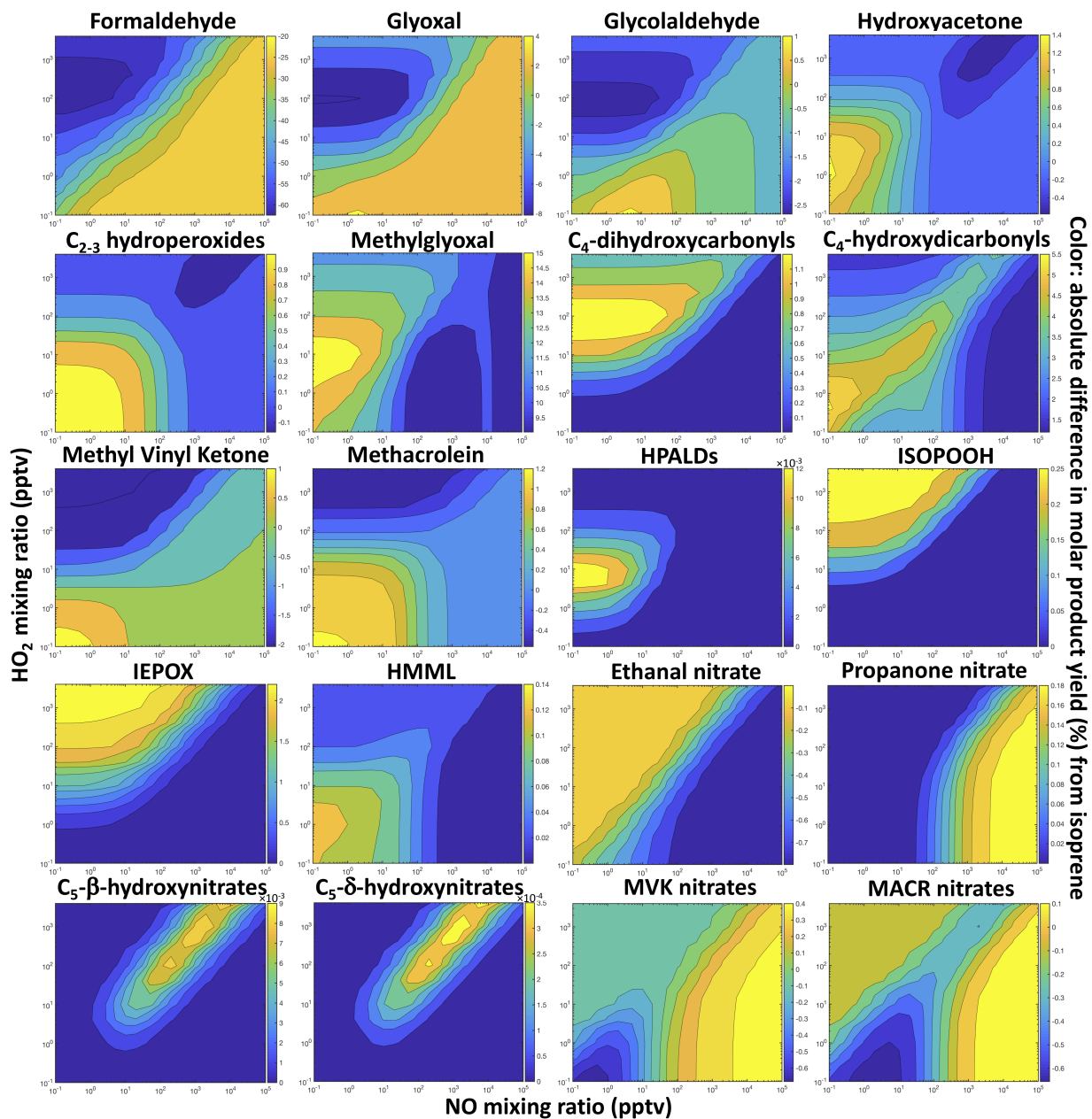
Figure S5: Absolute changes in percent yields of compounds of interest from isoprene when switching from fixed-radical box models with full photolytic sunlight flux (equatorial midday) to simulations with no photolytic light flux. All box models are run at 25 °C and using RCIM.

S3   Emission sensitivities in global models

Sensitivity simulations were performed with 10% increases and decreases to both isoprene and NO_x emissions worldwide, to examine the effects of these perturbations on the results reported herein. Changes in isoprene oxidation pathways due to emission changes can be found in Table S4, while changes in tropospheric average mixing ratios of species of interest can be found in Table S5. The contributions of isoprene oxidation pathways – including the initial oxidants, the ISOPOO fate, and the ISOPOO isomer reactivity – are largely insensitive to 10% perturbations in either NO_x or isoprene emissions, with the largest relative changes in the fraction of isoprene reacting with NO_3.

Table S4: Global contributions of isoprene oxidation pathways with changed isoprene and NO_x emissions.[a]

	Pathway	isoprene +10%	isoprene -10%	NO_x +10%	NO_x -10%	no anthro-pogenic NO_x	no anthrop. or BB NO_x
isop +	OH	87	88	88	88	89	90
	O_3	11	10	10	10	10	10
	NO_3	1.7	1.8	1.8	1.7	0.9	0.5
RO_2[b] +	HO_2	42	41	41	41	45	47
	NO	27	29	29	27	18	13
	RO_2	8.8	8.2	8.5	8.6	11	13
	H-shift	22	22	22	23	26	28
isomer	E/Z-1-OH-δ	6.5	6.5	6.4	6.5	7.5	8.0
	1-OH-β	59	59	59	59	58	58
	E/Z-4-OH-δ	14	14	14	14	16	16
	4-OH-β	21	21	21	21	19	18

[a]Reported percentages are global tropospheric annual averages, from $4° \times 5°$ horizontal resolution GEOS-Chem simulations using RCIM; numbers may not add to 100% due to rounding; [b]Referring only to the RO_2 radicals formed in the reaction of isoprene with OH and O_2.

Table S5: Changes in tropospheric burdens due to perturbations to isoprene and NO_x emissions (%)[a]

Species	isoprene +10%	isoprene -10%	NO_x +10%[b]	NO_x -10%[b]	no anthro-pogenic NO_x[b]	no anthrop. or BB NO_x[b]
OH	-0.42	0.82	1.6 (1.0)	-1.3 (-1.8)	-4.5 (-4.0)	-0.12 (0.86)
HO_2	0.32	-0.40	0.18 (0.50)	-0.27 (0.06)	-10 (-9.3)	-15 (-14)
NO	-0.27	0.41	2.8 (3.2)	-2.5 (-2.2)	-17 (-17)	-20 (-20)
NO_2	-0.21	0.13	5.1 (5.4)	-5.0 (-4.8)	-44 (-44)	-50 (-50)
NO_3	-0.42	0.38	3.8 (3.9)	-3.9 (-3.9)	-34 (-31)	-39 (-31)
O_3	0.21	-0.17	1.0 (0.63)	-1.0 (-1.3)	-16 (-15)	-20 (-19)
CO	1.2	-1.6	-1.1 (0.60)	0.84 (2.3)	-28 (-26)	-47 (-43)
Formaldehyde	1.0	-1.2	0.86 (0.68)	-1.1 (-1.2)	-14 (-13)	-15 (-13)
PANs[c]	1.0	-2.5	1.5 (2.0)	-3.0 (-1.9)	-54 (-53)	-62 (-61)
C_{2+} nitrates[c]	0.81	-2.4	1.4 (1.8)	-3.1 (-2.0)	-67 (-59)	-75 (-64)
Epoxides[c]	11	-11	-0.86	1.6	-22	-33
Tetrafunctionals[c]	4.4	-12	-5.0	-2.7	29	53
Isoprene SOA	15	-8	2.9	3.9	48	74
CH_4 lifetime	0.82	-0.59	-1.5 (-1.1)	1.9 (1.9)	9.8 (7.8)	6.3 (4.22)

[a]Percent differences are annual averages from $4° \times 5°$ horizontal resolution GEOS-Chem simulations using RCIM; [b]for simulations with changed NO_x emissions, numbers in parentheses are the percent change that results from the same change in NO_x emissions between two simulations with no isoprene emissions; [c]percent differences in lumped classes of compounds are calculated by mole, not mass.

S4   Isoprene oxidation at night

Figures S6-S10 show the results of diurnal-steady-state and fixed-radical simulations of nighttime isoprene chemistry, which was also updated substantially in Wennberg et al. (2018) following the recommendations of Schwantes et al. (2015). For diurnal-steady-state simulations, figures S6 and S7 show average mixing ratios of isoprene oxidation products over the period 20:00-04:00 on the seventh simulated night; in general, due to the persistence of isoprene + OH oxidation products, these exhibit on minimal differences from daytime averages. Notably, the diurnal-steady-state simulations do not include nighttime changes to the mixed layer height or depositional and aerosol-phase losses, which may cause substantial biases.

In fixed-radical simulations, a series of simulations investigating NO_3-initiated isoprene oxidation were performed alongside those investigating OH-initiated oxidation. They were run similarly to those described in Section 2.2 of the main text, but instead of initializing with 1 ppbv isoprene, they were initialized with 1 total ppbv of isoprene + NO_3 + O_2 peroxy radicals, distributed across the peroxy radical isomers as in Wennberg et al. (2018). RCIM does not include many reactions of NO_3 with stable isoprene oxidation products, because the rates and products of these reactions are poorly constrained. Instead, the mechanism emphasizes reactions of first-generation isoprene + NO_3 products with OH, which are expected to occur in the morning. The fixed-radical simulations were there run with 0.1 pptv OH and 10% of Equatorial midday light flux to target these morning conditions.

Figure S8 shows the yields of major products of isoprene + NO_3 oxidation as simulated in fixed-radical box models with RCIM, including functionalized nitrates and the epoxides produced in their reactions with OH (Jacobs et al., 2014; Schwantes et al., 2015). Figure S9 compares these yields to those of fixed-radical simulations using the MCM v3.3.1 isoprene oxidation mechanism, which exhibits much higher formation of carbonyl nitrates and much lower production of C_4 nitrates, ethanal nitrate, and epoxides. Figure S10 compares RCIM to the GEOS-Chem v11-02c mechanism in fixed-radical nighttime simulations. The GEOS-Chem mechanism includes a smaller pool of functional products from isoprene + NO_3 oxidation, with high yields of C_5 hydroxy- and hydroperoxy-nitrates and only minor yields of the other products shown in RCIM.
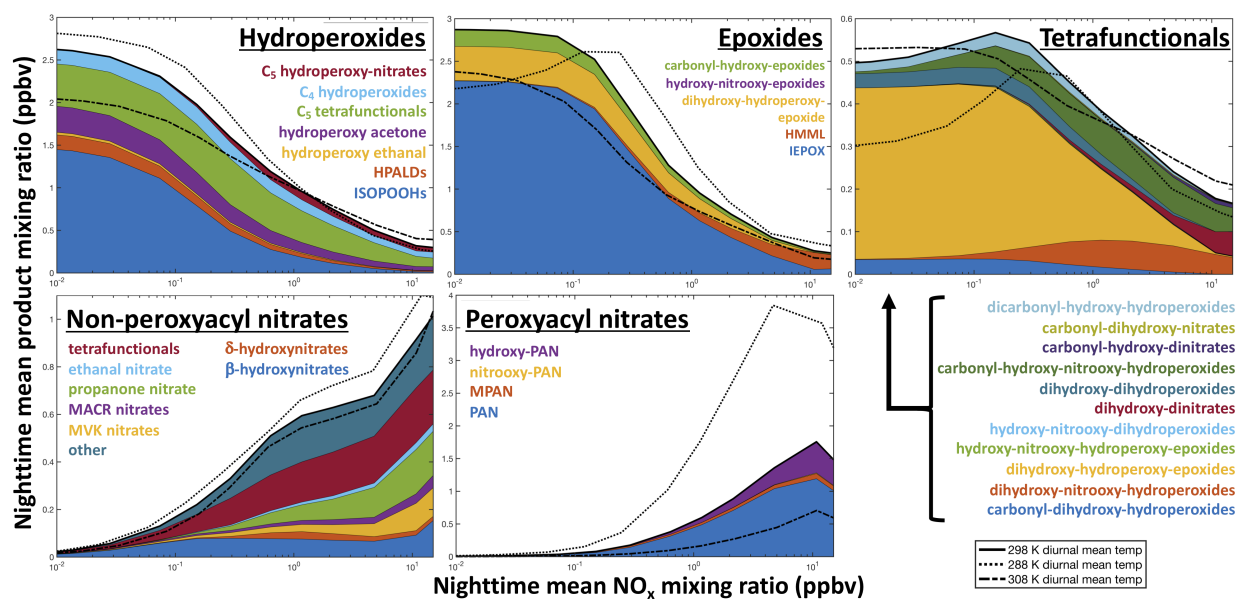
Figure S6: Nighttime average mixing ratios of major classes of compounds from isoprene oxidation in diurnal-steady-state box models as functions of NO_x and temperature, using RCIM. Y axis scales vary between graphs.
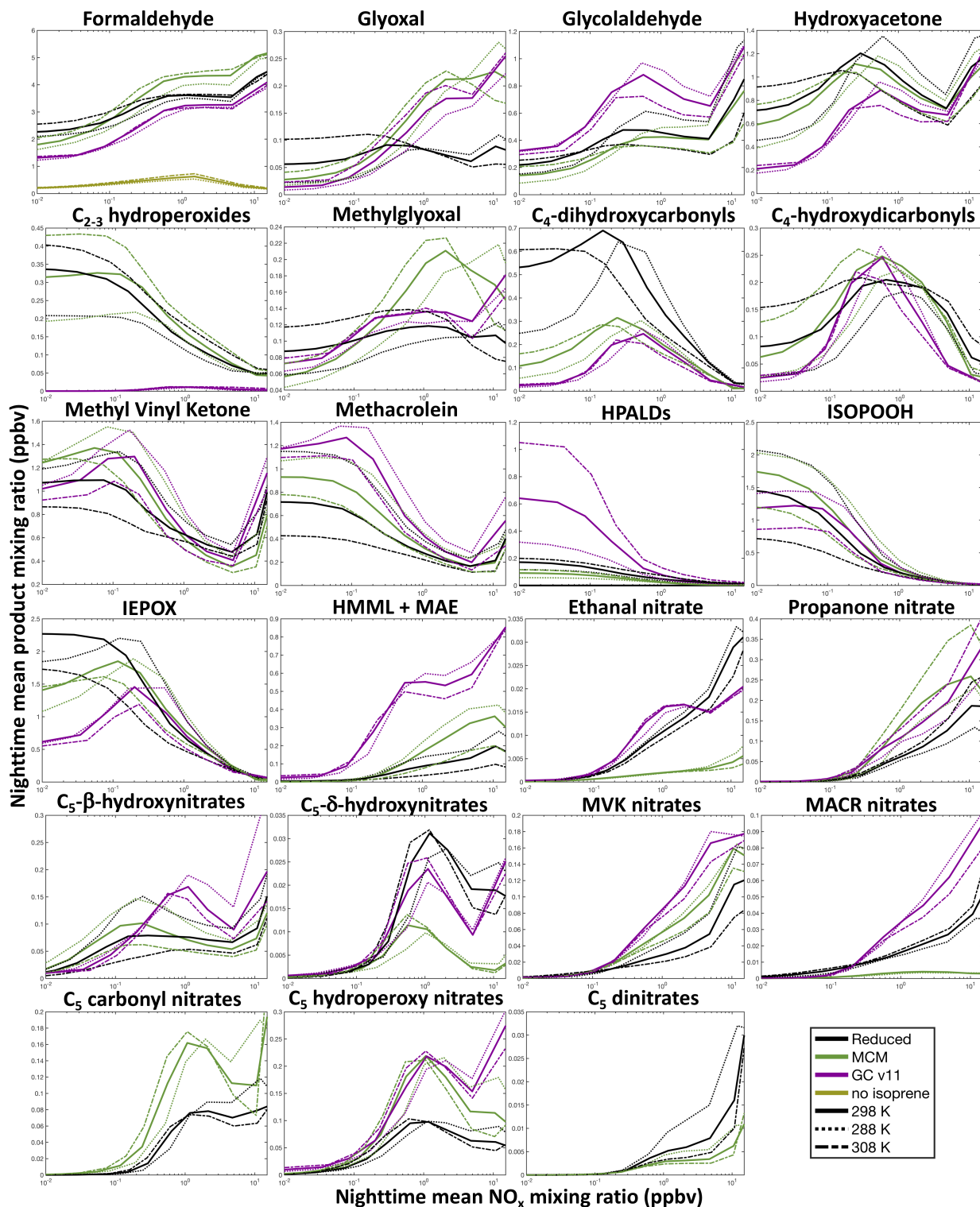
Figure S7: Nighttime average mixing ratios of major products of isoprene oxidation in diurnal-steady-state box models as functions of NO$_x$ and temperature, using RCIM. Y axis scales vary between graphs. For formaldehyde, the model assumes a background mixing ratio of 300 pptv, with some additional contribution from methane oxidation. For HPETHNL + HPAC, ¡10% of the total is contributed by HPETHNL under all conditions.
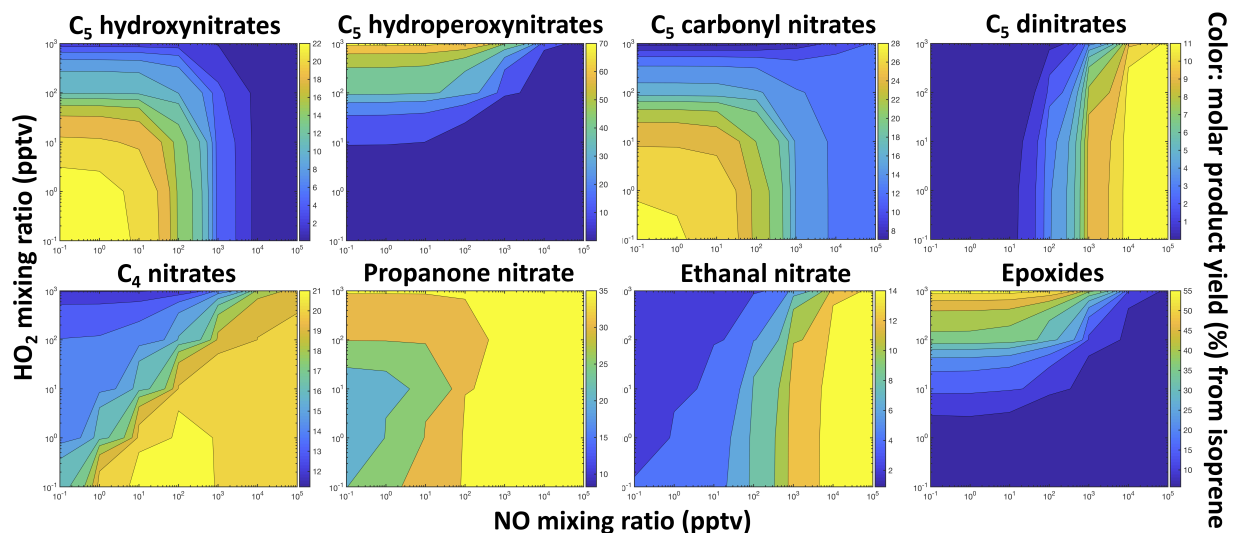
Figure S8: Percent yields of compounds of interest from isoprene + NO₃ oxidation in RCIM. All box models are run at 25 °C and 10% of equatorial midday photolytic light flux.
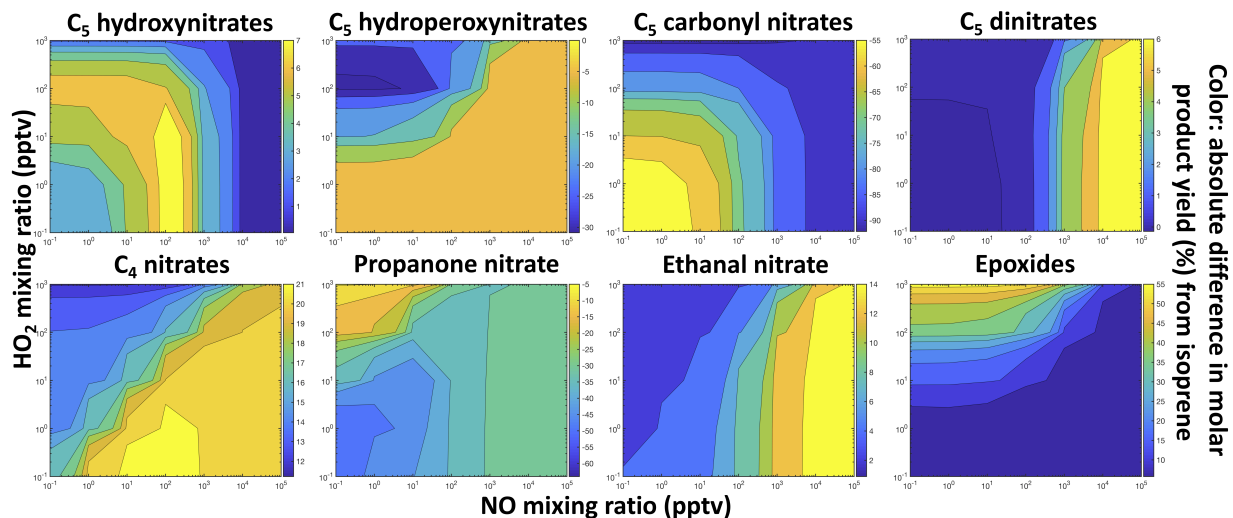
Figure S9: Absolute changes in percent yields of compounds of interest from isoprene + NO₃ oxidation when switching from fixed-radical box models with the MCM v3.3.1 mechanism (Jenkin et al., 2015) to RCIM. All box models are run at 25 °C and 10% of equatorial midday photolytic light flux.

S5   Comparisons to other mechanisms

Figures S11-S24 and Tables S3 and S6 show detailed comparisons between RCIM, MCM v3.3.1, and the GEOS-Chem v11-02c isoprene oxidation mechanisms in box models, and between RCIM and v11-02c in global simulations. Many differences between the mechanisms stem from variability in the initial reactive pathway branching of isoprene, shown in Section S5.1, and from differences between the OH-recycling tendencies of the mechanisms under low-NO conditions (Section S5.2). These differences then carry over into variability in the yields of organic products (Section S5.3).
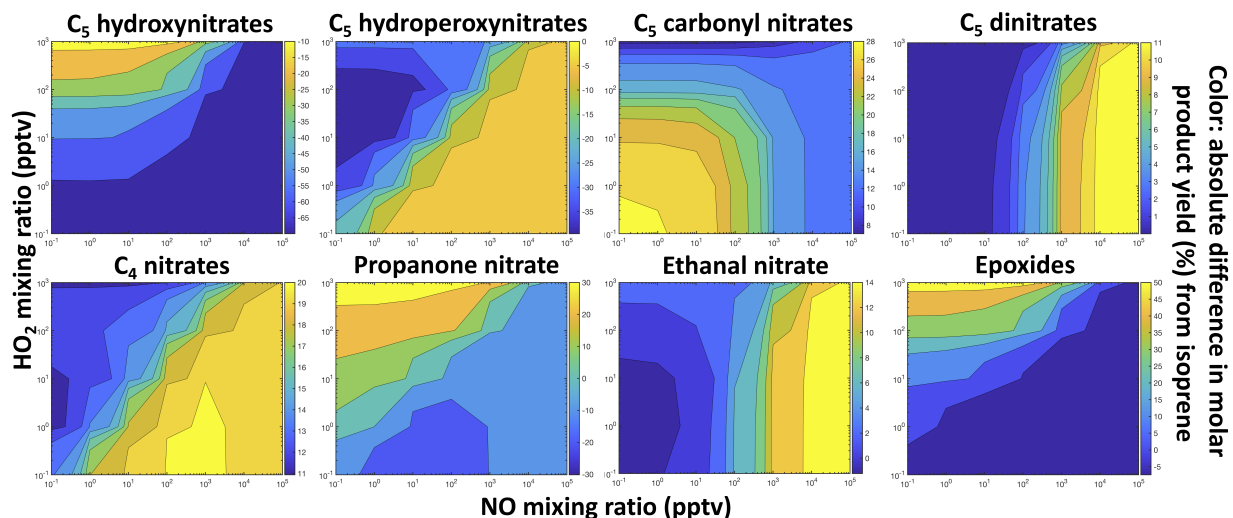
Figure S10: Absolute changes in percent yields of compounds of interest from isoprene + NO_3 oxidation when switching from fixed-radical box models with the GEOS-Chem v11-02c mechanism to RCIM. All box models are run at 25 °C and 10% of equatorial midday photolytic light flux.

S5.1 Isoprene reaction pathways

Figure S11 shows the contributions of specific reactive pathways to the overall fate of isoprene in diurnal-steady-state box models with the three isoprene oxidation mechanisms. Lower OH recycling under low-NO conditions in the MCM and GEOS-Chem mechanisms relative to RCIM means that less OH is available to react with isoprene, and leads to a higher reactivity with ozone, by up to a factor of 2 in the MCM mechanism and over a factor of 3 in the GEOS-Chem v11-02c mechanism. This effect is also visible in global chemical transport simulations with RCIM and v11-02c (Figure S12). The increased OH recycling in RCIM also sustains higher HO_2 mixing ratios, which leads to a larger fraction of ISOPOO reacting with HO_2 than in the other mechanisms. Fixed-radical simulations (Figure S13 and S14) show that when NO and HO_2 are held constant, RCIM results in a larger proportion of ISOPOO reacting via H-shifts than the other two mechanisms, and only deviates substantially from MCM in the fraction reacting via each isomer under extremely high-NO conditions.

S5.2 HO_x, NO_x, and ozone

Figures S15 and S16 show the differences in net production of HO_x, NO_x and ozone due to isoprene oxidation by the three different mechanisms in fixed-radical box models. As described in the main manuscript, the main difference between the mechanisms is the higher HO_x recycling in RCIM under conditions where H-shift chemistry dominates. This can also be seen in global simulations comparing GEOS-Chem v11-02c and RCIM (Figure S17 and Table S6), which show that RCIM sustains OH concentrations up to three times those of the GEOS-Chem v11-02c mechanism in remote regions of high isoprene emission such as the Amazon, and that the reduced MPAN formation rate in RCIM leads to much lower NO_x titration over the Amazon.
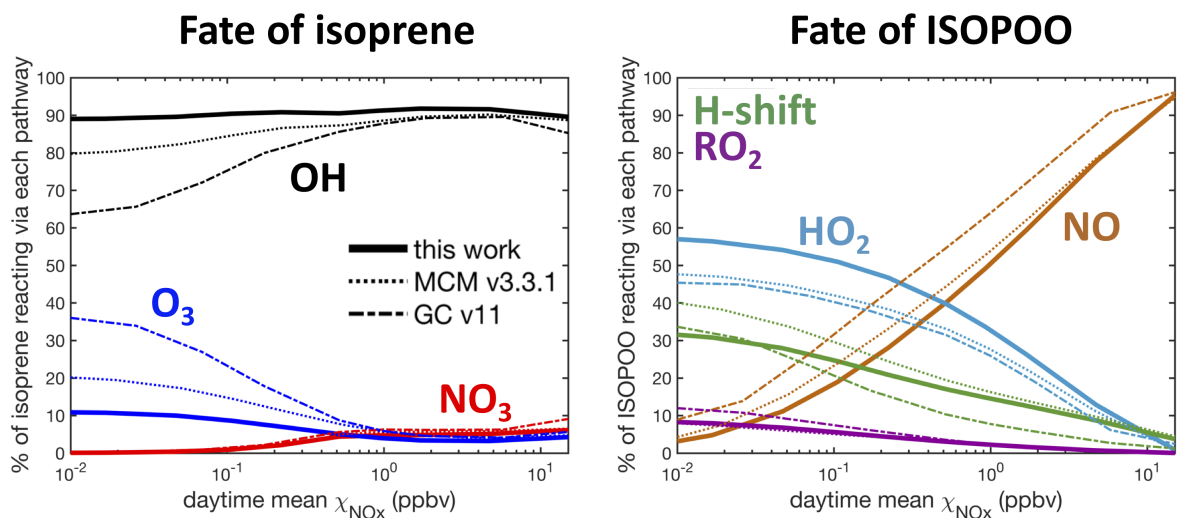
Figure S11: Isoprene oxidation pathway branchings in diurnal-steady-state box models as a function of NO_x mixing ratio, using RCIM (solid), MCM v3.3.1 (dashed), and GEOS-Chem v11-02c (dotted).
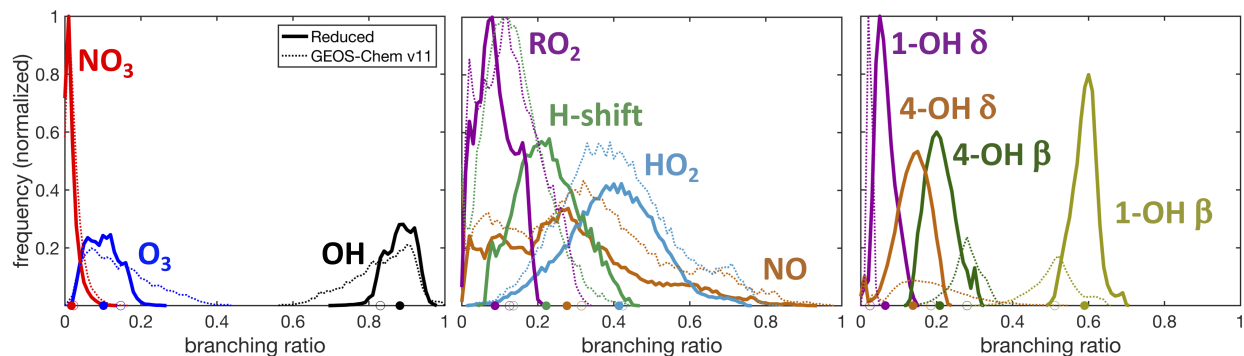

Figure S12: Isoprene oxidation pathway branchings in GEOS-Chem using RCIM (solid lines, filled dots) and GEOS-Chem v11-02c (dotted lines, open dots), at $2° \times 2.5°$ horizontal resolution, on an annual average. The curves represent probability density functions of the models grid boxes, weighted by the amount of isoprene reacting in each grid box, while the dots on the x axis represent the global annual total reacting via each pathway.
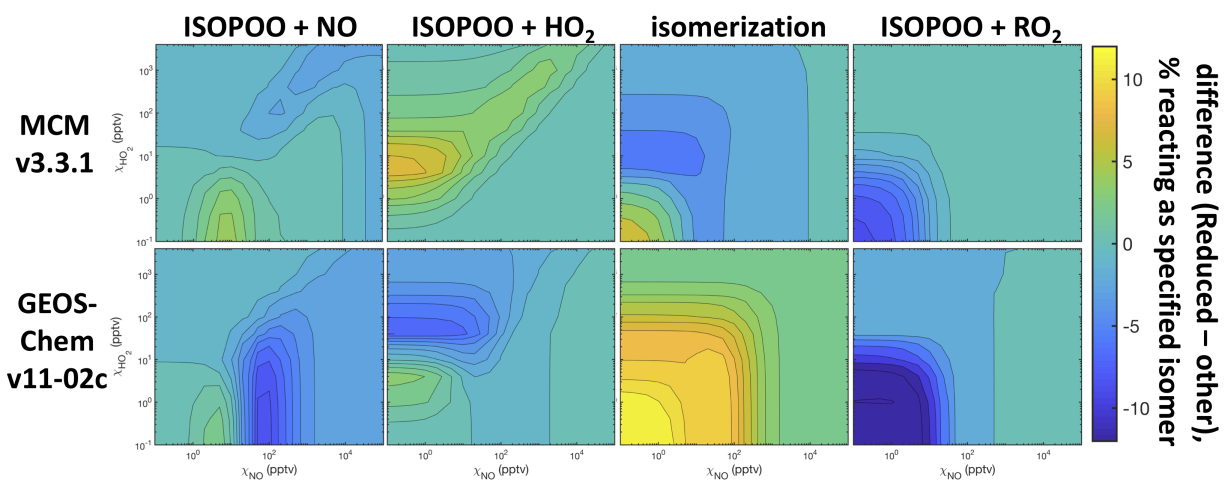
Figure S13: Absolute difference between RCIM and MCM v3.3.1 (top) and GEOS-Chem v11-02c (bottom) in the percent of isoprene hydroxy peroxy radicals reacting via each pathway as a function of NO and HO_2, from fixed-radical box modeling of all three mechanisms at 298 K and full photolytic sunlight flux (equatorial midday).
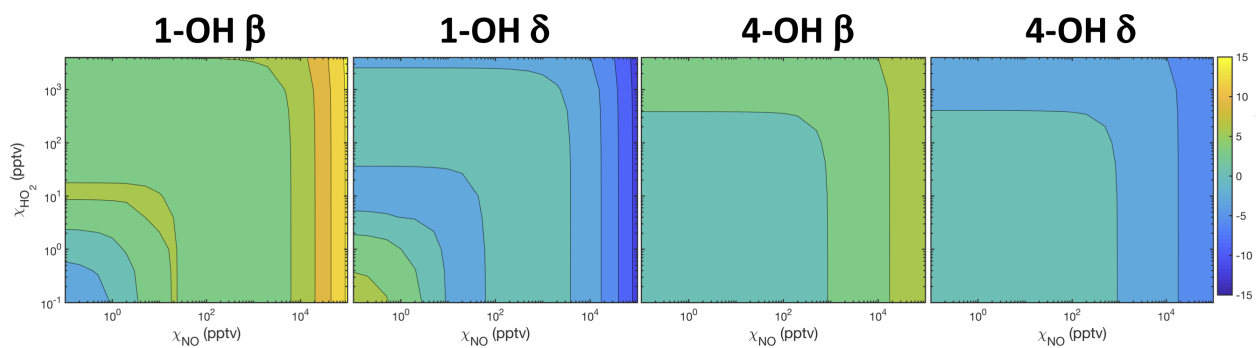

Figure S14: Absolute difference between RCIM and MCM v3.3.1 mechanism in the percent of isoprene hydroxy peroxy radicals reacting via each isomer as a function of NO and HO_2, from fixed-radical box modeling of all three mechanisms at 298 K and full photolytic sunlight flux (equatorial midday).

Table S6: Differences (%) in annual average mixing ratios between GEOS-Chem simulations using RCIM and the GEOS-Chem v11-02c mechanism[a]

species	troposphere	0-1 km	5-10 km	SE USA[b]	Amazon[b]	E China[b]
OH	1.2[c]	-0.57	-0.70	-12	-63	-3.3
HO_2	2.0	0.75	1.9	-0.41	-24	-0.26
NO	-2.4	0.27	-3.9	2.2	0.2	-0.45
NO_2	0.69	0.97	-2.8	1.7	-16	0.44
NO_3	6.6	4.3	-1.5	-1.5	-26	2.7
O_3	2.5	2.7	1.8	1.5	14	1.0
CO	-1.1	-1.4	-0.90	-1.7	-8.2	-0.22
HCHO	-0.99	-7.0	3.8	-11	-44	-1.4
Formicacid	9.3	-14	59	-23	-48	-9.8
Aceticacid	-14	-23	3.6	-30	-42	-24
Glycolaldehyde	60	42	130	27	100	-6.3
Glyoxal	130	87	430	310	47	26
Hydroxyacetone	1.3	-11	43	-0.40	-47	12
Methylglyoxal	8.9	-5.6	83	7.4	-43	6.5
Methyl vinyl ketone	-5.5	-17	52	-7.9	-34	-12
Methacrolein	33	19	105	26	-1.8	20
C_4 dihydroxycarbonyls	-34	-47	30	-48	-65	-36
PANs[d]	50	34	52	39	400	7.8
C_{2+} nitrates[d,e]	160	240	68	220	1100	86
C_5 nitrates[d]	490	360	420	270	700	230
C_5 hydroxynitrates	640	530	440	450	870	470
C_4 nitrates[d]	860	700	1300	410	1500	300
Propanone nitrate	120	100	87	100	100	71
C_{2+} hydroperoxides[d]	65	33	360	29	11	31
ISOPOOH	25	0.035	370	16	-25	13
C_5 hydroperoxy aldehydes	400	290	1100	140	330	62
Epoxides[d]	96	34	420	38	-30	120
IEPOX	29	-1.0	190	5.2	-41	24
HMML	900	630	1600	430	780	360
Tetrafunctionals[d]	2500	1800	2900	980	2600	2300
SOA	-39	-61	48	-75	-81	-33

[a]Results from $2° \times 2.5°$ horizontal resolution global simulations. Positive percentages indicate higher mixing ratios in GEOS-Chem v11-02c than RCIM. [b]Average mixing ratios from 0-1 km altitude. [c]Causing a 1.16% decrease in the tropospheric methane lifetime. [d]Yields of lumped species may include multiple generations of a single oxidation pathway (e.g., separately counting both IEPOX and its oxidation product, isoprene hydroxycarbonyl epoxides). [e]Includes only non-PAN organonitrates.
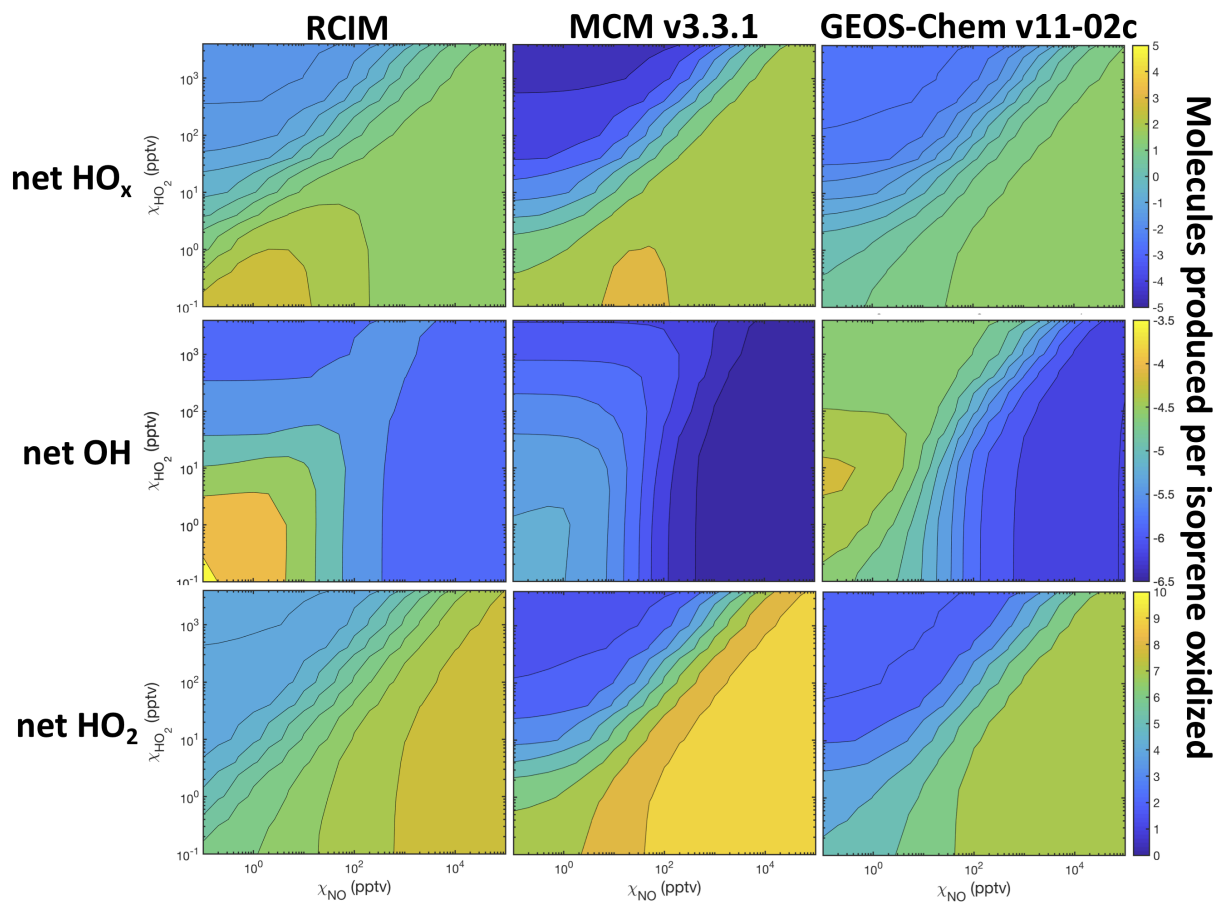
Figure S15: Net molar production or consumption of HO_x, OH, and HO_2 from isoprene oxidation as a function of NO and HO_2 in RCIM (top), MCM v3.3.1 (middle) and GEOS-Chem v11-02c (bottom), from fixed-radical box modeling of all three mechanisms at 298 K and full photolytic sunlight flux (equatorial midday).
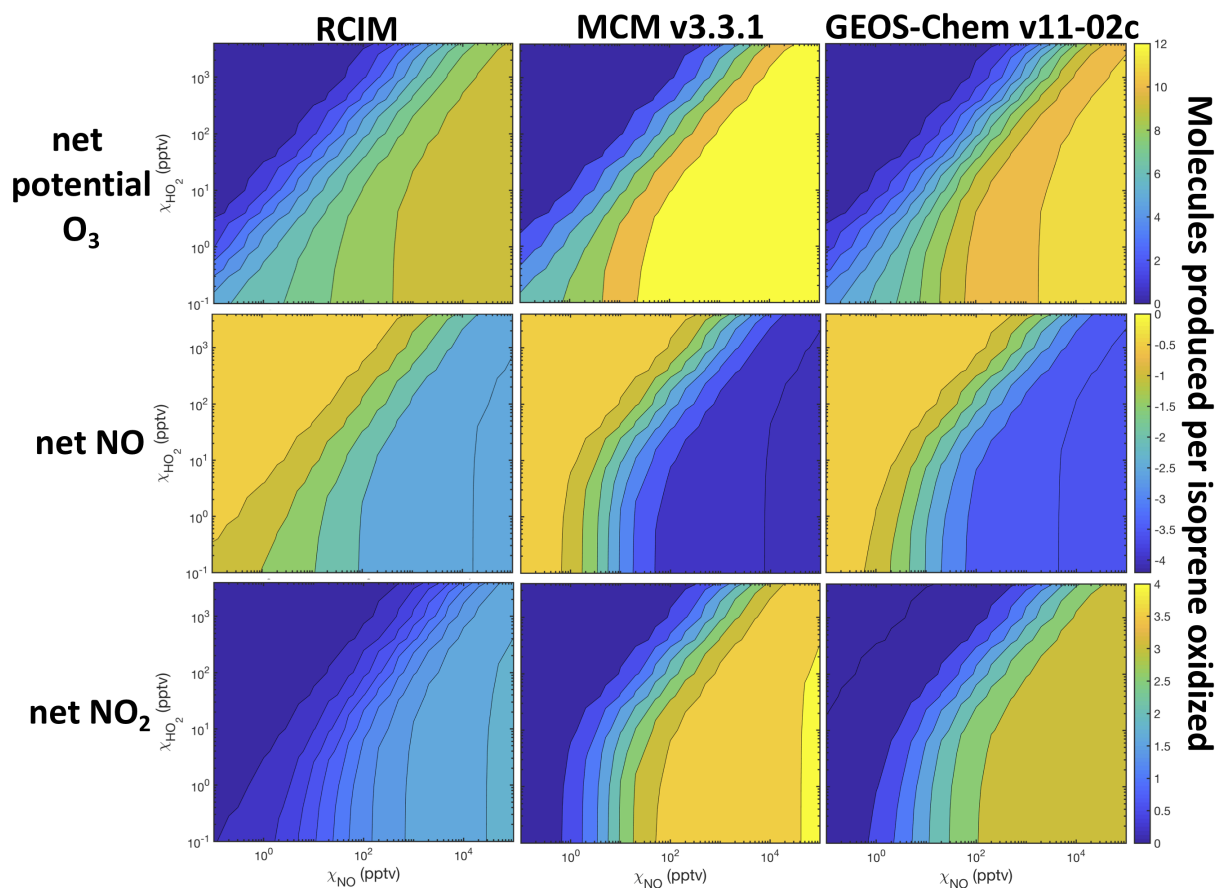
Figure S16: Net molar production or consumption of potential O_3, NO, and NO_2 from isoprene oxidation as a function of NO and HO_2 in RCIM (top), MCM v3.3.1 (middle) and GEOS-Chem v11-02c (bottom), from fixed-radical box modeling of all three mechanisms at 298 K and full photolytic sunlight flux (equatorial midday). Net potential O_3 is estimated as the sum of net production of ozone, NO_2, and HO_2 (times the fraction of HO_2 that would go on to react with NO based on the relative concentrations of its potential reaction partners).
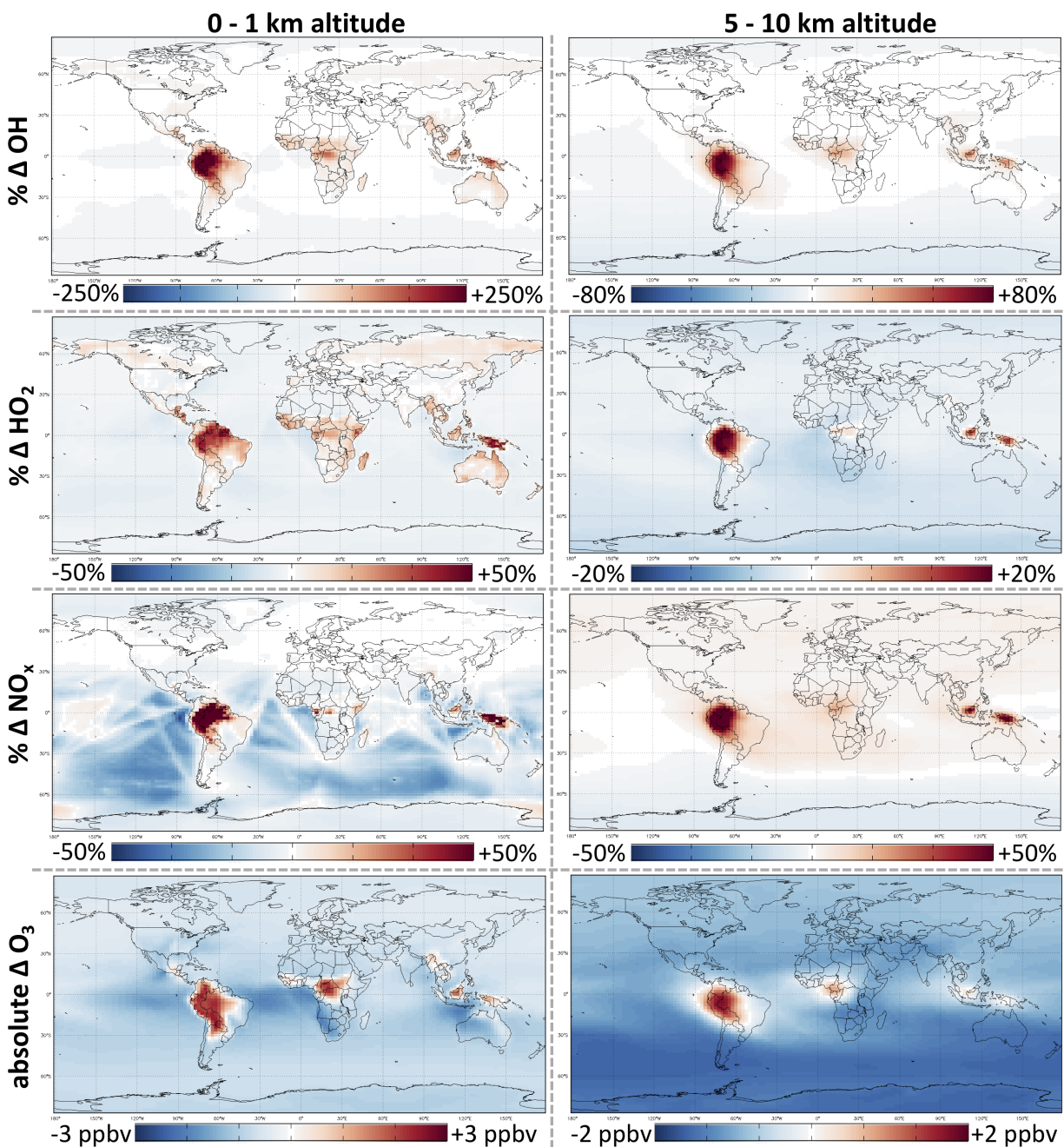
Figure S17: Changes in annual average mixing ratios of OH, HO$_2$, NO$_x$, and O$_3$ from a $2° × 2.5°$ horizontal resolution GEOS-Chem simulation with the GEOS-Chem v11-02c mechanism to one with RCIM.

S5.3 Organic products

Figures S18 and S19 show the differences in yields of organic products between RCIM, MCM v3.3.1, and GEOS-Chem v11-02c in fixed-radical box model simulations. Figures S20-S23 show differences in daytime mixing ratios of organic products between the mechanisms in diurnal-steady-state simulations. Table S3 shows differences in mean annual yields of organic isoprene oxidation products between GEOS-Chem v11-02c and RCIM in global chemical transport simulations, while Figure S24 and Table S6 show differences in mean

annual mixing ratios of organic isoprene oxidation products from the same simulations. The maps in Figure S24 show the higher formaldehyde production from local isoprene oxidation over remote forests as well as the strong effects of the decreased MPAN formation rate in RCIM, along with smaller corresponding decreases in PAN formation and in the lifetimes of tertiary nitrates due to rapid hydrolysis. The major differences between product yields are noted in the main manuscript; these figures are provided as a reference for those seeking a more detailed accounting of individual products.
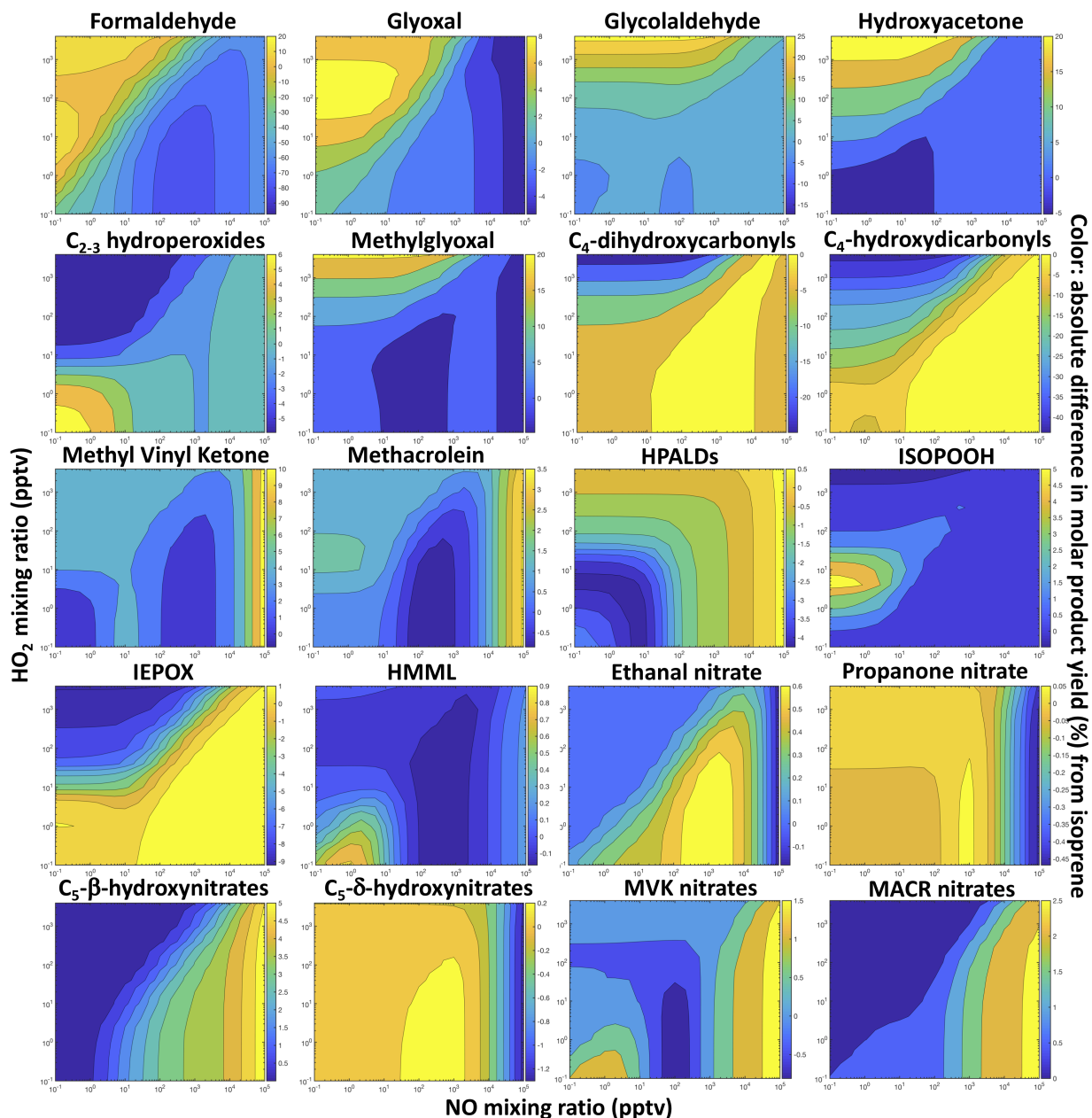

Figure S18: Absolute changes in percent yields of compounds of interest from isoprene + OH oxidation when switching from fixed-radical box models with MCM v3.3.1 (Jenkin et al., 2015) to RCIM. All box models are run at 25 °C and equatorial midday photolytic light flux.
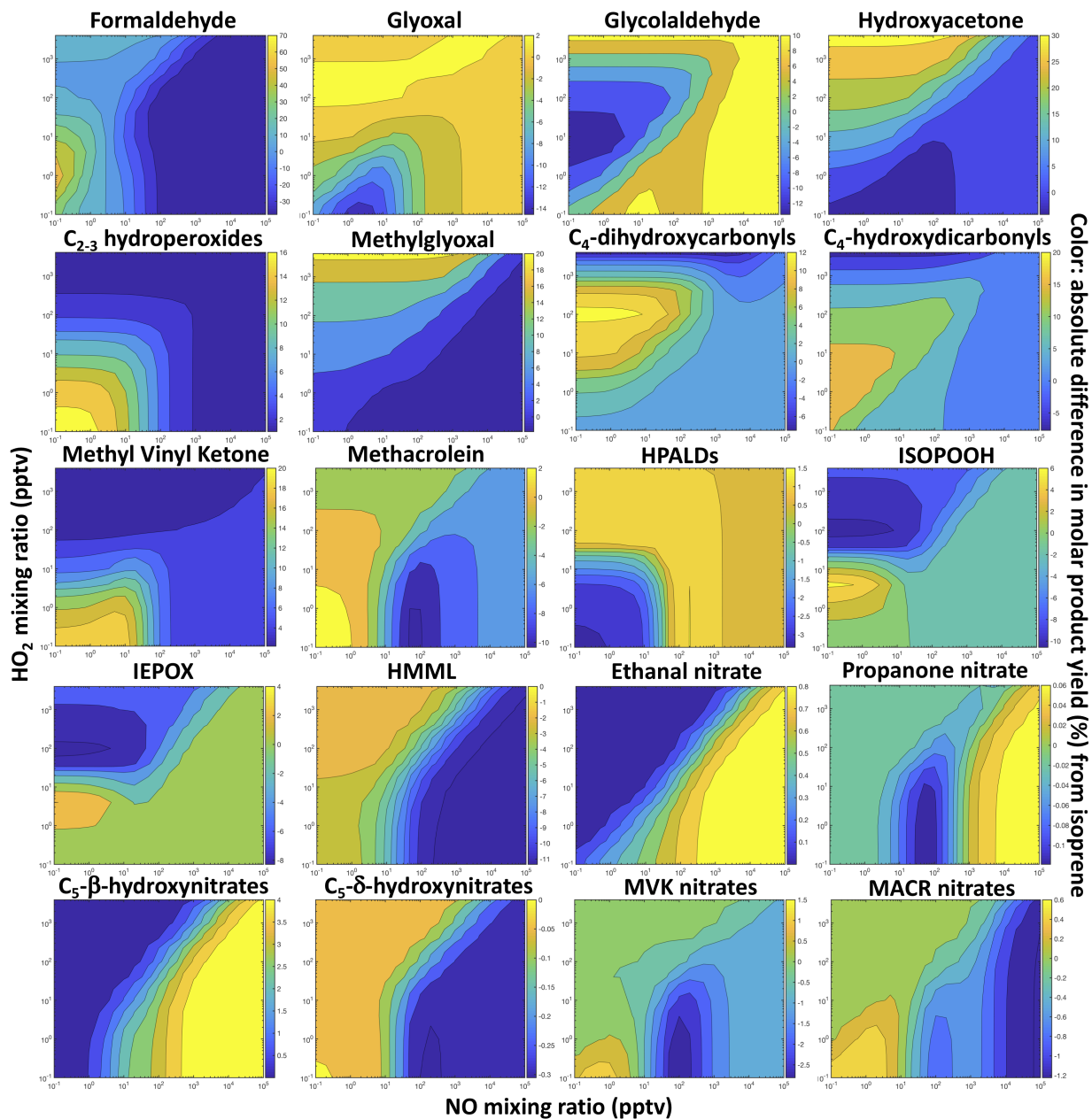
Figure S19: Absolute changes in percent yields of compounds of interest from isoprene + OH oxidation when switching from fixed-radical box models with GEOS-Chem v11-02c to RCIM. All box models are run at 25 °C and equatorial midday photolytic light flux.
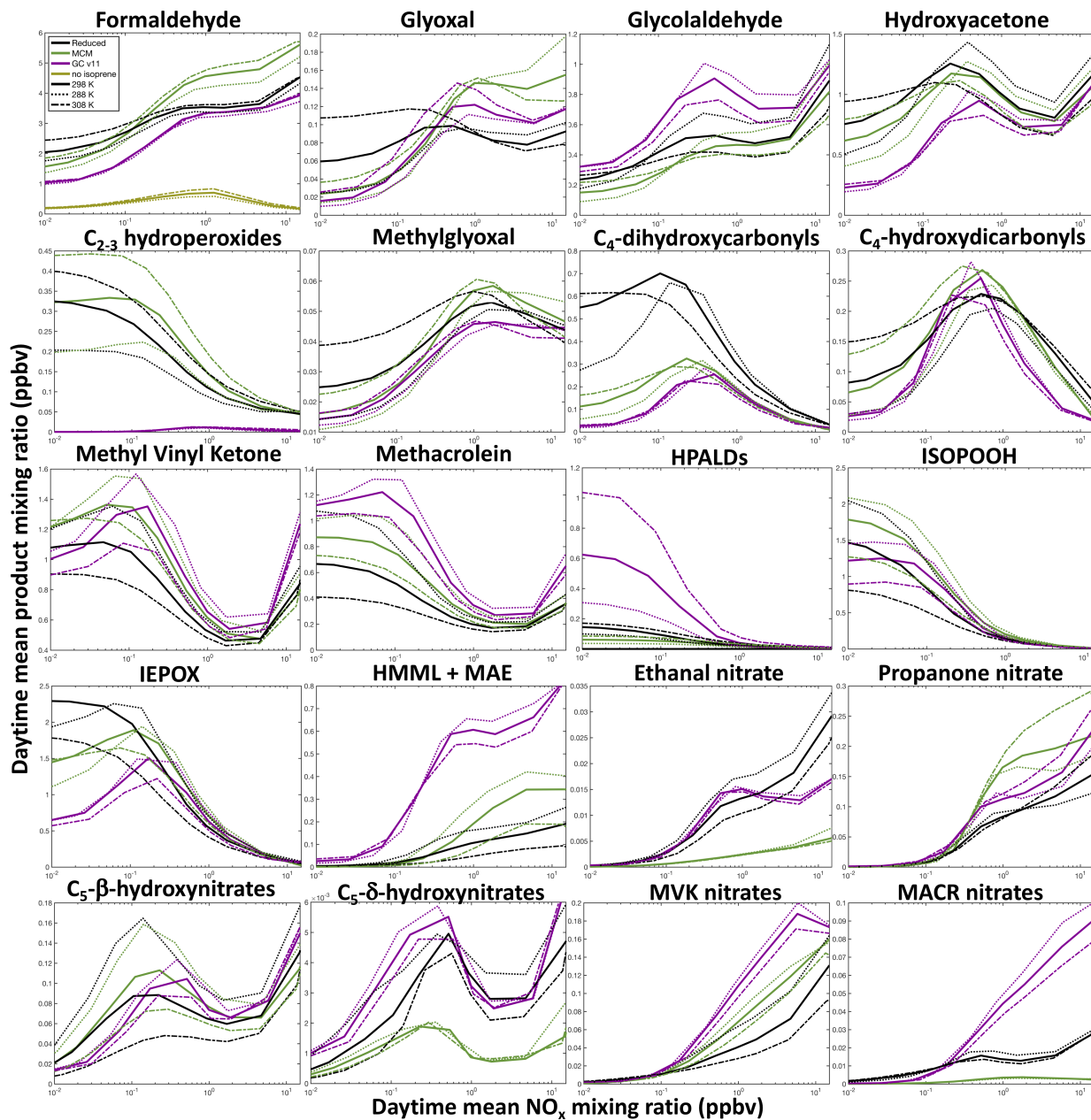
Figure S20: Daytime average mixing ratios of isoprene oxidation products in diurnal-steady-state box models as a function of NO$_x$ mixing ratio (X axis) and temperature (line style), using RCIM (black), MCM v3.3.1 (green), and GEOS-Chem v11-02c (purple).
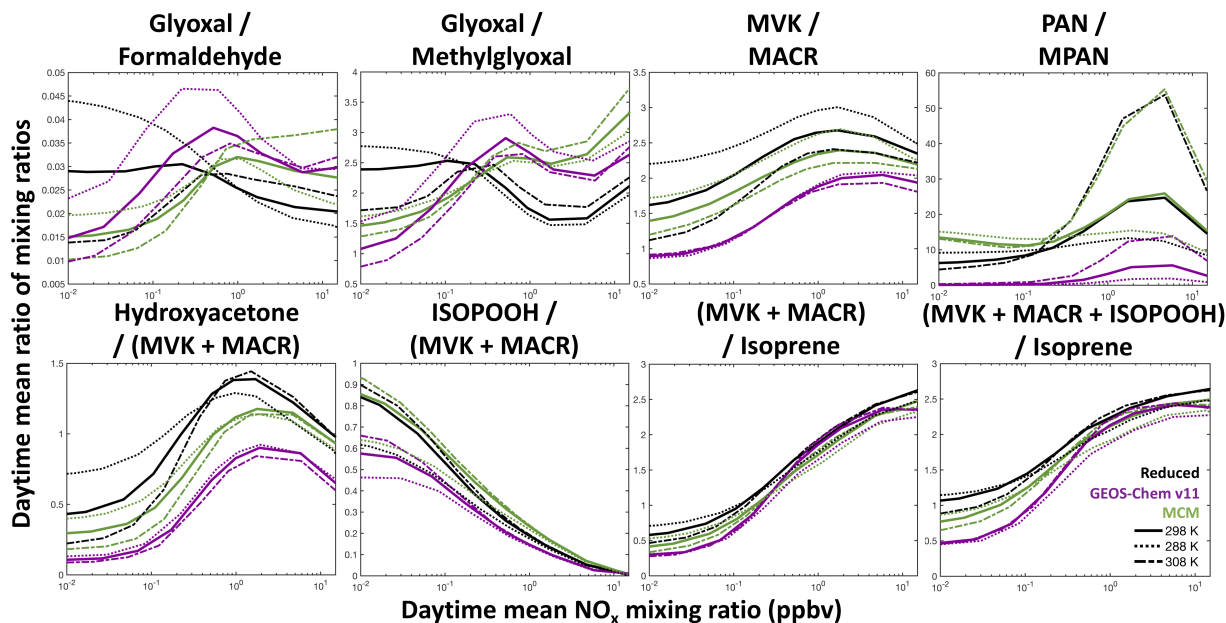
Figure S21: Commonly reported ratios between daytime average mixing ratios of isoprene oxidation products in diurnal-steady-state box models as a function of NO_x mixing ratio (X axis) and temperature (line style), using RCIM (black), MCM v3.3.1 (green), and GEOS-Chem v11-02c (purple).

Figure S22: Daytime average mixing ratios of major classes of compounds from isoprene oxidation in diurnal-steady-state box models as functions of NO_x (X axis) and temperature (black lines), using MCM v3.3.1. Y axis scales vary between graphs. Grey lines denote corresponding mixing ratios using the RCIM for comparison.
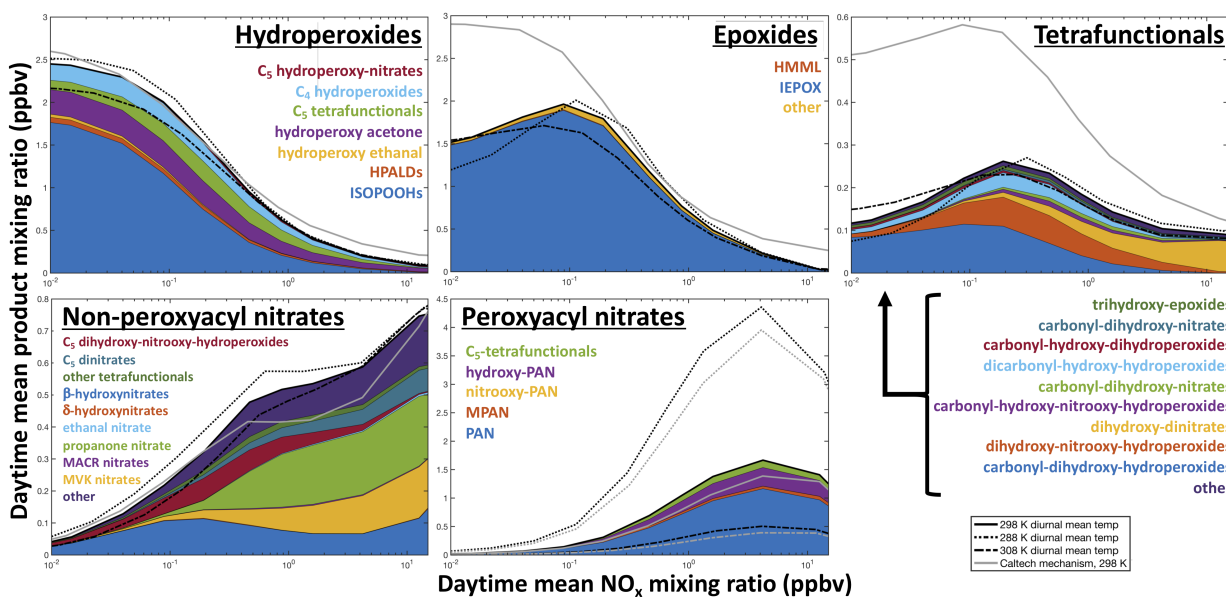
Figure S23: Daytime average mixing ratios of major classes of compounds from isoprene oxidation in diurnal-steady-state box models as functions of NO_x (X axis) and temperature (black lines), using GEOS-Chem v11-02c. Y axis scales vary between graphs. Grey lines denote corresponding mixing ratios using RCIM for comparison.

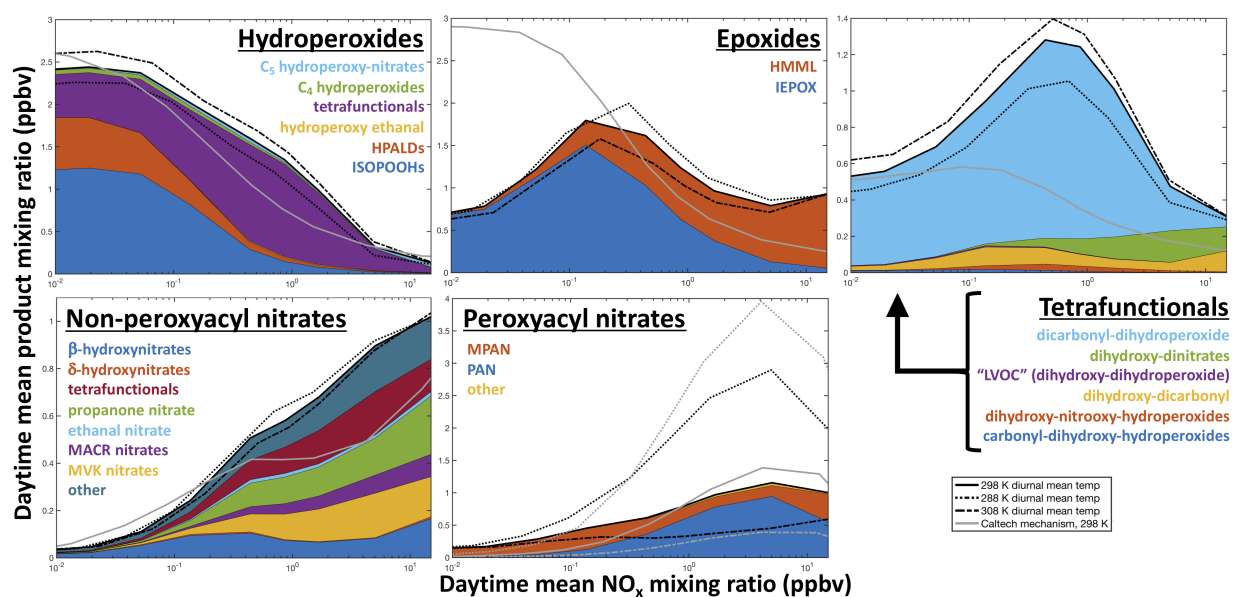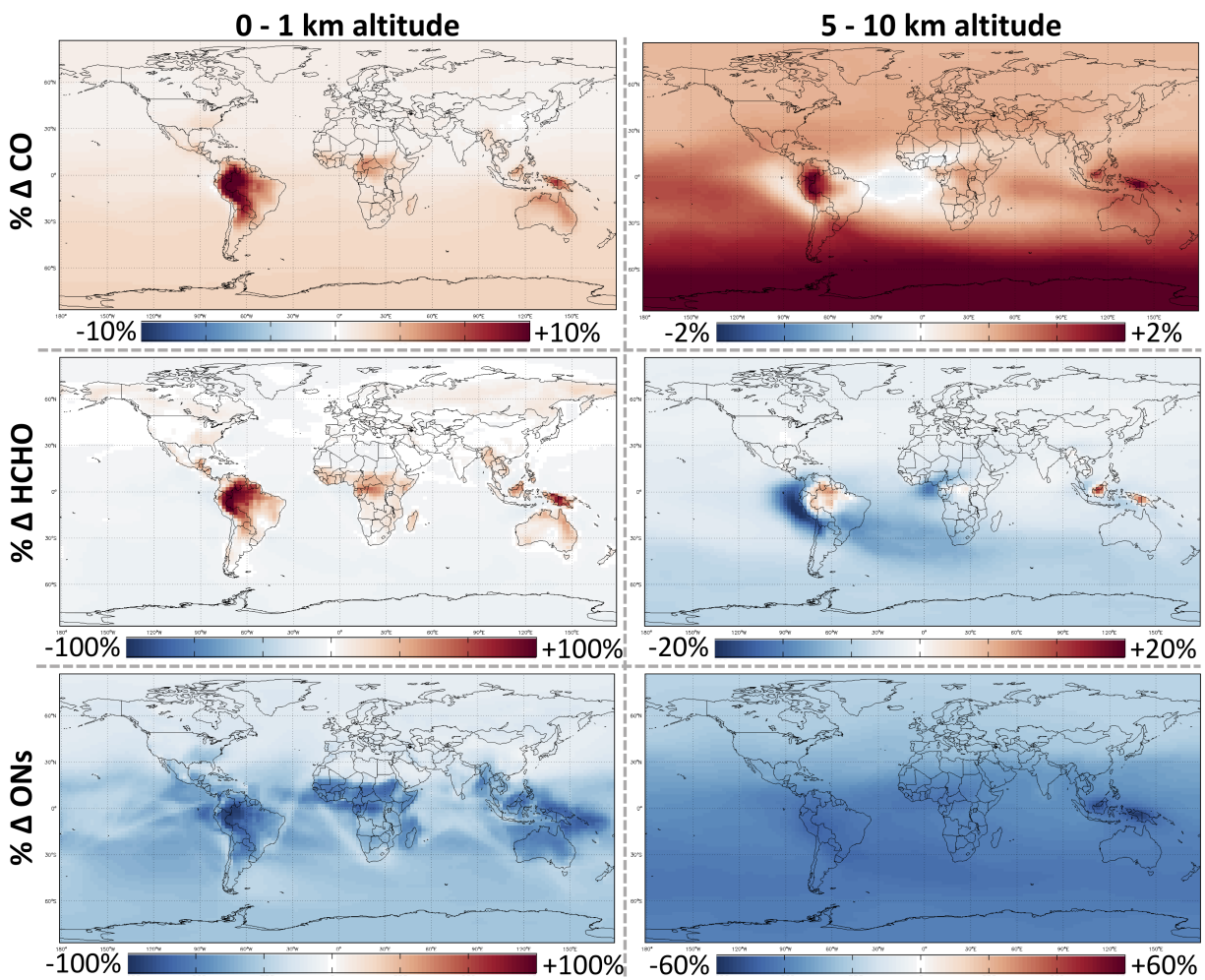Figure S24: Percent changes in annual average mixing ratios of CO (top), formaldehyde (middle), and total organonitrates (bottom) from a $2° \times 2.5°$ horizontal resolution GEOS-Chem simulation with the GEOS-Chem v11-02c mechanism to one with RCIM.

S6 Mechanism simplification

Table S7 provides the differences in tropospheric and regional production and mixing ratios of species between annual GEOS-Chem simulations using RCIM and Mini-CIM. As described in the main text, the changes between the two mechanisms are minimal (~ 0.1 %), particularly for HO_x, NO_x, O_3, CO, and HCHO. Larger reductions in C_{2+} organonitrate (2.8 %) and C_5 tetrafunctional (12 %) production are largely due to the removal of multigenerational steps (e.g. the conversion of one tetrafunctional species into another), and therefore do not carry over substantially to changes in mixing ratios. Further, the moderate percent reduction (4.4 %) in mixing ratios of organonitrates over the Amazon represents only a tiny absolute difference, since the region experiences very little nitrate formation.

Table S7: Differences (%) in annual production and mixing ratios between GEOS-Chem simulations using RCIM and Mini-CIM

species	tropospheric production	tropospheric loading	loading, 0-1 km	loading, Amazon	loading, SE USA	loading, E China
OH	-	-0.14	-0.12	-0.17	-0.03	-0.01
HO_2	-	-3.2E-3	-0.022	-0.020	0.079	0.025
NO_x	-	-0.17	-0.02	-0.22	0.020	0.016
O_3	-	-0.11	-0.097	-0.42	-0.074	-0.028
CO	-0.11	-0.078	0.054	0.038	0.014	5.1E-3
HCHO	-0.13	-0.096	-0.11	-0.12	-0.13	-0.047
GLYC	-0.66	-0.53	-0.67	-0.63	-0.68	-0.30
GLYX	0.43	0.58	0.47	-1.2	2.1	0.076
HAC	0.14	0.089	0.33	0.55	-0.24	-0.42
MGLY	-0.35	-0.17	-0.077	-0.11	0.22	0.084
PANs	-	-0.34	-0.18	-0.50	-0.28	-0.067
C_{2+}nitrates[a]	-2.8	-0.68	0.77	4.4	2.4	0.02
C_{2+}hydroperoxides	-0.65	0.43	0.44	0.14	1.4	2.9
epoxides	1.7E-3	0.32	0.21	0.11	0.28	0.38
SOA	0.17	0.23	0.082	-0.10	0.17	0.023
C_5tetrafunctionals	-12	-0.048	-0.21	-0.074	-0.64	2.2

[a]Includes only non-PAN organonitrates

Table S8 shows the annual global and regional molar product yields from isoprene of species removed from RCIM to create Mini-CIM. We also provide a complete list of the simplifications made to create Mini-CIM below. Naming conventions follow those laid out in Wennberg et al. (2018) and used in RCIM. More details, along with a complete listing of the reactions and species in both RCIM and Mini-CIM, can be found online in the mechanism repository (DOI 10.22002/D1.247)

The following simplifications apply to species that meet the simplification criteria of $< 0.1\%$ yield from isoprene globally and $< 1\%$ yield from isoprene regionally in the Amazon, the southeastern United States, and eastern China:

- ISOP3CO4OH is replaced with ISOP1OH2OO3CO4OH; because ISOP3CO4OH + OH = ISOP1OH-2OO3CO4OH + OH is the only loss process of ISOP3CO4OH, this replacement is OH-neutral.

- The acylperoxy radical of hydroxyethane ($HOCH_2C(O)OO\bullet$) is replaced with the peroxyacetyl radical ($CH_3C(O)OO\bullet$), and the products of its reactions with HO_2 and NO_2 ($HOCH_2C(O)OOH$, $HOCH_2C(O)OH$, and $HOCH_2C(O)OONO_2$) are removed.

- The acylperoxy radical of nitrooxyethane ($O_2NOCH_2C(O)OO\bullet$) is replaced with the peroxyacetyl radical ($CH_3C(O)OO\bullet$) plus NO_2, and the products of its reactions with HO_2 and NO_2 ($O_2NOCH_2C(O)OOH$, $O_2NOCH_2C(O)OH$, and $O_2NOCH_2C(O)OONO_2$) are removed.

- The three isoprene carbonyl nitrate isomers are lumped into a single species (ICN) representing 70% ISOP1N4CO, 30% ISOP1CO4N, and 0% ISOP3CO4N, the proportion in which they are produced in GEOS-Chem simulations; the subsequent reaction rates and products of the single ICN species are scaled according to these proportions.

- ICN3OO (ISOP1OH2OO3CO4N) is removed, as it is no longer produced from IC3N.

- ICN1OO (ISOP1N2OH3OO4CO) and ICN2OO (ISOP1CO2OO3OH4N) are found to undergo rapid H-shifts under almost all ambient conditions (Möller et al., 2019), and are therefore replaced with the H-shift products.

- The acylperoxy radical products of ICN + OH are lumped into a single species (ICNOO) representing 70% ICN4OO (ISOP1N4CO4OO) and 30% ICN5OO (ISOP1CO1OO4N), the proportions in which they are produced in GEOS-Chem simulations; the subsequent reaction rates and products of the single ICNOO species are scaled according to these proportions.

- MVK-derived nitrates are lumped into a single species (MVKN) representing 69% MVK3N4OH, 29% MVK3OH4N, 1% MVK3OOH4N, and 1% MVK3CO4N, the proportions in which they are produced in GEOS-Chem simulations; the subsequent reaction rates and products of the single MVKN species are scaled according to these proportions.

- MACR1OOH2N3OH is replaced with MACR2N3OH, which has nearly identical subsequent reactions.

- Minor isomers of methacrolein-derived nitrates are lumped into a single species (MACRN) representing 75% MACR2OH3N, 25% MACR2OOH3N, and 0% MACR1OH2N3OH, the proportions in which they are produced in GEOS-Chem simulations; the subsequent reaction rates and products of the single MACRN species are scaled according to these proportions.

- All dinitrates are lumped into a single species (IDN) representing 50% dihydroxy-dinitrates (IDHDN), 50% dinitrates retaining a double bond (IDN), 0% isoprene-hydroxy-hydroperoxy-dinitrates (IHPDN), and 0% isoprene-carbonyl-hydroxy-dinitrates (ICHDN), the proportions in which they are produced in GEOS-Chem simulations; the subsequent reaction rates and products of the single IDN species are scaled according to these proportions.

- All tri- and tetra-functionalized C_5 hydroxynitrates are lumped into a single species (ITHN) representing 90% isoprene-dihydroxy-hydroperoxy-nitrate (IDHPN), 10% isoprene-hydroxy-nitrooxy- epoxide (IHNE), 0% isoprene-hydroxy-dihydroperoxy-nitrates (IHNDP), and 0% isoprene-hydroxy-hydroperoxy-nitrooxy-epoxides (IHNPE), the proportions in which they are produced in GEOS-Chem simulations; the subsequent reaction rates and products of the single ITHN species are scaled according to these proportions. Because the hydroxy-nitrates have similar photolytic and OH loss pathways, this combination minimizes changes to the species' lifetimes.

- Isoprene-carbonyl-nitrooxy-epoxides (ICNE) and isoprene-dihydroxy-carbonyl-nitrates (IDHCN) are replaced with isoprene-carbonyl-hydroxy-hydroperoxy-nitrates (ICHNP), which is renamed as ITCN to reflect the lumped isoprene tri- and tetra-functionalized carbonyl nitrates. Because the carbonyl-nitrates have similar photolytic and OH loss pathways, this combination minimizes changes to the species' lifetimes.

- IHNEOO, the peroxy radical from isoprene-hydroxy-nitrooxy-epoxides (IHNE) + OH, is replaced with the peroxy radical from NO_3-derived beta-hydroxy nitrates + OH (IDHNBOO), which reacts similarly.

- The lumped β-hydroxynitrates from isoprene + NO3 oxidation (IHNB) are combined with the lumped beta-hydroperoxynitrates from isoprene + NO_3 oxidation (INPB); the subsequent reaction rates and products of the single INPB species are scaled (33% IHNB, 67% INPB) according to the proportions in which they are produced in GEOS-Chem simulations.

- Hydroxy-nitrooxy-methacryloylperoxynitrate (MPANHN) is replaced with methacryloylperoxynitrate (MPAN) + NO2.

- The acid (MACR1OH) and peracid (MACR1OOH) from the methacryloylperoxy radical reaction with HO2 are lumped into a single species (MACR1OOH) representing 75% MACR1OOH and 25% MACR1OH, the proportions in which they are produced in GEOS-Chem simulations; the subsequent reaction rates and products of the single ITHN species are scaled according to these proportions.

- SOA from methylglyoxal (SOAMG) and from HMML (SOAME) are combined, respectively, with SOA from glyoxal (SOAGX) and IEPOX (SOAIE). This simplification applies only to GEOS-Chem, not the gas-phase mechanism found in the online repository.

The following simplifications apply to species that do not meet the yield criteria described above, but are isobaric and have the same loss rates, such that combining them does not affect the species' atmospheric lifetime:

- ISOP1CO4OH and ISOP1OH4CO are lumped into a single C_5-δ-hydroxy-carbonyl species (HC5) representing 65% ISOP1CO4OH and 35% ISOP1OH4CO, the proportions in which they are produced in GEOS-Chem simulations; the subsequent reaction rates and products of the single HC5 species are scaled according to these proportions.

- MVKENOL and MCRENOL are lumped into a single C_4-enol species (MCRENOL) representing 75% MCRENOL and 25% MVKENOL, the proportions in which they are produced in GEOS-Chem simulations; the subsequent reaction rates and products of the single enol species are scaled according to these proportions.

- MACR2OH3CO and MVK3OH4CO have identical reaction pathways, and are therefore lumped into a single C_4-hydroxy-dicarbonyl species (MVKHCB).

- MACR2OOH3OH and MACR2OH3OOH are lumped into a single hydroxy-hydroperoxy-methacrolein species (MACRHP) representing 77% MACR2OOH3OH and 23% MACR2OH3OOH, the proportions in which they are produced in GEOS-Chem simulations; the subsequent reaction rates and products of the single MACRHP species are scaled according to these proportions.

- MVK3OOH4OH and MVK3OH4OOH are lumped into a single hydroxy-hydroperoxy-MVK species (MVKHP) representing 53% MVK3OOH4OH and 47% MVK3OH4OOH, the proportions in which they are produced in GEOS-Chem simulations; the subsequent reaction rates and products of the single MVKHP species are scaled according to these proportions.

Table S8: Annual mean molar yields (%) from isoprene of species removed from the simplified mechanism[a]

species	global	Amazon	SE USA	E China
$HOCH_2CO_2H$	1.7E-4	1.9E-6	1.8E-5	1.2E-5
$HOCH_2CO_3H$	3.3E-4	2.4E-6	3.1E-5	2.1E-5
$O_2NOCH_2CO_2H$	5.8E-4	2.0E-5	3.7E-4	5.6E-4
$O_2NOCH_2CO_3H$	9.3E-4	2.5E-5	6.2E-4	9.3E-4
$O_2NOCH_2CO_3NO_2$	0.012	2.6E-4	0.017	0.080
$HOCH_2CO_3NO_2$	8.7E-4	1.1E-5	6.7E-4	9.9E-4
MPANHN	0.018	1.5E-3	0.037	0.049
MVK3OOH4N	6.9E-3	5.6E-4	0.013	0.023
MVK3CO4N	5.2E-3	1.7E-4	7.6E-3	0.011
MACR2OOH3N	0.023	1.3E-3	0.045	0.059
MACR1OH2N3OH	2.2E-3	7.3E-4	1.5E-3	7.3E-4
MACR1OOH2N3OH	2.5E-3	6.8E-4	2.1E-3	1.2E-3
ISOP3CO4OH	0.069	0.037	0.059	0.036
ISOP1CO4N	0.088	8.2E-3	0.21	0.32
ISOP3CO4N	9.1E-3	7.8E-4	0.024	0.024
dinitrooxy-isoprene	0.035	4.0E-3	0.092	0.20
nighttime β-hydroxynitrates	0.053	4.9E-3	0.13	0.13
C_5 dihydroxy-dinitrates	0.035	2.1E-3	0.068	0.17
C_5 hydroxy-hydroperoxy-dinitrates	2.1E-3	6.8E-5	2.9E-3	1.3E-3
C_5 carbonyl-hydroxy-dinitrates	1.3E-3	3.7E-6	3.9E-4	8.0E-4
C_5 hydroxy-nitrooxy-epoxides	0.027	2.1E-3	0.037	0.013
C_5 hydroxy-nitrooxy-dihydroperoxides	5.4E-3	3.9E-4	4.7E-3	1.0E-3
C_5 hydroxy-nitrooxy-hydroperoxy-epoxides	2.0-E-3	2.5E-4	3.3E-3	8.0E-4
C_5 carbonyl-nitrooxy-epoxides	1.4E-3	2.5E-5	6.1E-4	2.6E-4
C_5 carbonyl-dihydroxy-nitrates	0.011	1.5E-4	3.9E-3	7.6E-3
MVK3OH4N[b]	0.17	0.015	0.21	0.48
ISOP1OH4CO[b]	0.31	0.24	0.38	0.57
MVK3OH4OOH[b]	2.5	1.1	1.3	1.1
MVKENOL[b]	0.37	0.65	0.22	0.12
MACR2OH3CO[b]	0.25	0.026	0.12	0.13
MACR2OH3OOH[b]	0.24	0.13	0.20	0.24
MACR1OH[b]	0.36	0.25	0.14	0.064
SOA from HMML/MAE[c]	0.023	2.6E-3	7.9E-3	0.030
SOA from methylglyoxal[c]	2.1E-3	2.0E-3	2.1E-3	0.015

[a]Species names are derived from Wennberg et al. (2018) and the mechanism posted in the online repository; [b]While these species' yields exceed the threshold set for exclusion, their lifetimes and loss pathways are sufficiently similar to those of other species in the mechanism to facilitate their combination (see text); [c]These simplification applies only to GEOS-Chem, not the gas-phase mechanism found in the online repository.

References

Arey, J., Aschmann, S. M., Kwok, E. S., and Atkinson, R.: Alkyl nitrate, hydroxyalkyl nitrate, and hydroxycarbonyl formation from the NO_x-air photooxidations of C_5-C_8 n-alkanes, J. Phys. Chem. A, 105, 1020–1027, https://doi.org/10.1021/jp003292z, 2001.

Carter, W. P. L. and Atkinson, R.: Atmospheric chemistry of alkanes, J. Atmos. Chem., 3, 377–405, https://doi.org/10.1007/BF00122525, 1985.

Carter, W. P. L. and Atkinson, R.: Alkyl nitrate formation from the atmospheric photoxidation of alkanes: A revised estimation method, J. Atmos. Chem., 8, 165173, https://doi.org/10.1007/BF00053721, 1989.

Crounse, J. D., Paulot, F., Kjaergaard, H. G., and Wennberg, P. O.: Peroxy radical isomerization in the oxidation of isoprene, Phys. Chem. Chem. Phys., 13, 13607–13613, https://doi.org/10.1039/C1CP21330J, 2011.

Jacobs, M. I., Burke, W. J., and Elrod, M. J.: Kinetics of the reactions of isoprene-derived hydroxynitrates: Gas phase epoxide formation and solution phase hydrolysis, Atmos. Chem. Phys., 14, 8933–8946, https://doi.org/10.5194/acp-14-8933-2014, 2014.

Jenkin, M. E., Young, J. C., and Rickard, A. R.: The MCM v3.3.1 degradation scheme for isoprene, Atmos. Chem. Phys., 15, 11433–11459, https://doi.org/10.5194/acp-15-11433-2015, 2015.

Mao, J., Paulot, F., Jacob, D. J., Cohen, R. C., Crounse, J. D., Wennberg, P. O., Keller, C. A., Hudman, R. C., Barkley, M. P., and Horowitz, L. W.: Ozone and organic nitrates over the eastern United States: Sensitivity to isoprene chemistry, J. Geophys. Res., 118, 11256–11268, https://doi.org/10.1002/jgrd.50817, 2013.

Möller, K. H., Bates, K. H., and Kjaergaard, H. G.: The importance of peroxy radical hydrogen-shift reactions in atmospheric isoprene oxidation, J. Phys. Chem. A, 123, 920–932, https://doi.org/10.1021/acs.jpca.8b10432, 2019.

Paulot, F., Crounse, J. D., Kjaergaard, H. G., Kroll, J. H., Seinfeld, J. H., and Wennberg, P. O.: Isoprene photooxidation: New insights into the production of acids and organic nitrates, Atmos. Chem. Phys., 9, 1479–1501, https://doi.org/10.5194/acp-9-1479-2009, 2009.

Peeters, J. and Nguyen, T. L.: Unusually fast 1,6-H shifts of enolic hydrogens in peroxy radicals: Formation of the first-generation C_2 and C_3 carbonyls in the oxidation of isoprene, J. Phys. Chem. A, 116, 6134–6141, https://doi.org/10.1021/jp211447q, 2012.

Peeters, J., Muller, J. F., Stavrakou, T., and Nguyen, V. S.: Hydroxyl radical recycling in isoprene oxidation driven by hydrogen bonding and hydrogen tunneling: The upgraded LIM1 mechanism, J Phys. Chem. A, 118, 8625–8643, https://doi.org/10.1021/jp5033146, 2014.

Praske, E., Otkjær, R. V., Crounse, J. D., Hethcox, J. C., Stoltz, B. M., Kjaergaard, H. G., and Wennberg, P. O.: Atmospheric autoxidation is increasingly important in urban and suburban North America, Proc. Natl. Acad. Sci., 115, 64–69, https://doi.org/10.1073/pnas.1715540115, 2018.

Schwantes, R. H., Teng, A. P., Nguyen, T. B., Coggon, M. M., Crounse, J. D., Clair, J. M. S., Zhang, X., Schilling, K. A., Seinfeld, J. H., and Wennberg, P. O.: Isoprene NO_3 oxidation products from the RO_2 + HO_2 pathway, J. Phys. Chem. A, 119, 10158–10171, https://doi.org/10.1021/acs.jpca.5b06355, 2015.

Wennberg, P. O., Bates, K. H., Crounse, J. D., Dodson, L. G., McVay, R. C., Mertens, L. A., Nguyen, T. B., Praske, E., Schwantes, R. H., Smarte, M. D., St Clair, J. M., Teng, A. P., Zhang, X., and Seinfeld, J. H.: Gas-phase reactions of isoprene and its major oxidation products, Chem. Rev., 118, 3337–3390, https://doi.org/10.1021/acs.chemrev.7b00439, 2018.